Sub-Ice Thermal Regime, Volcanogenic Processes and Terrane Assembly in Antarctica Using Magnetotellurics

Phil Wannamaker, Graham Hill, Virginie Maris,
John Stodt, Yasuo Ogawa, Michal Kordy
Univ. of Utah, Univ. of Canterbury, Tokyo Inst. of Technology

U.S. National Science Foundation, U.S. Department of Energy, Royal Society of New Zealand

Bedrock Topography, Antarctica
Fretwell et al (2013)

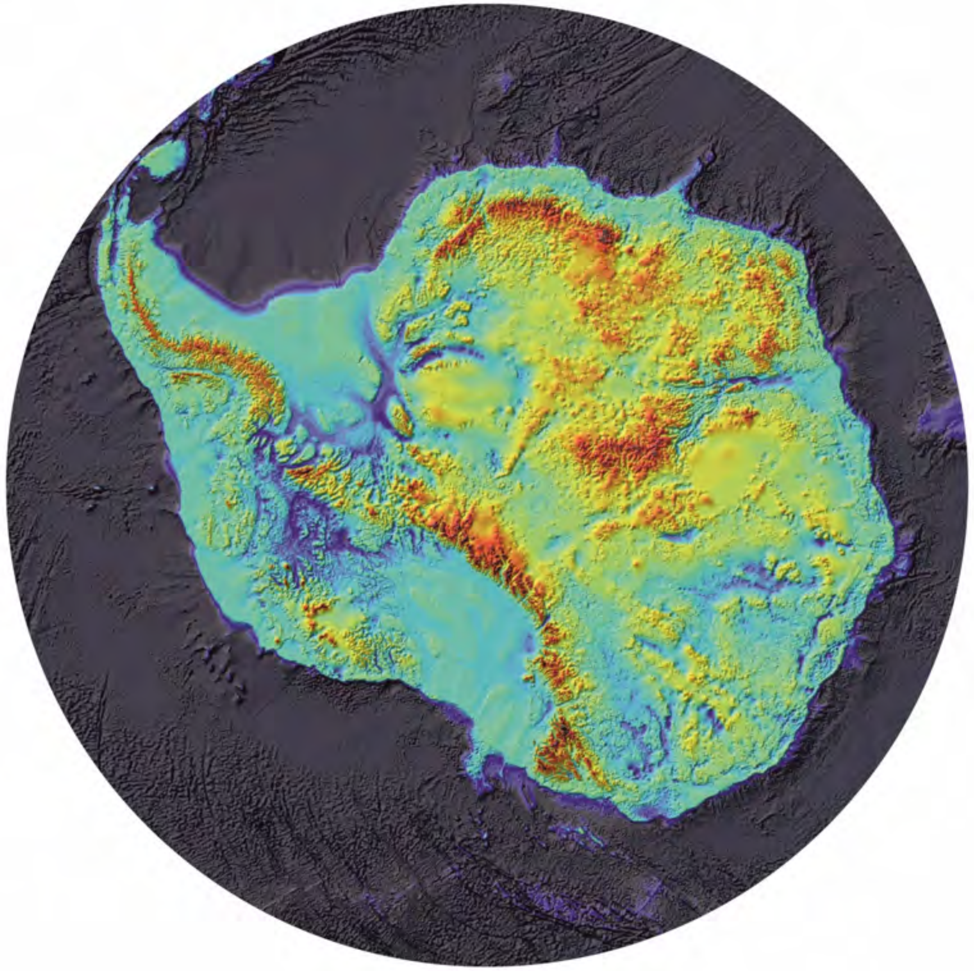

Subduction/Backarc Rifting and Continental Growth

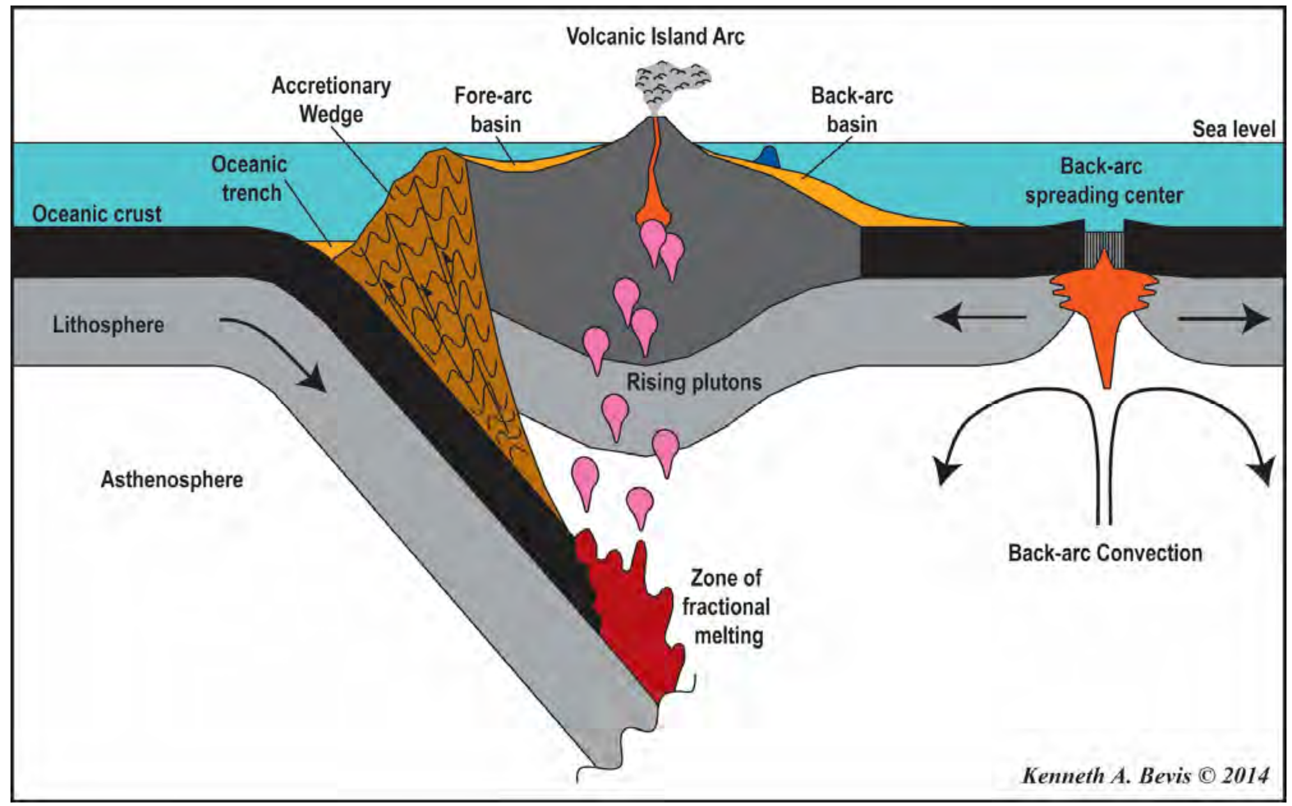

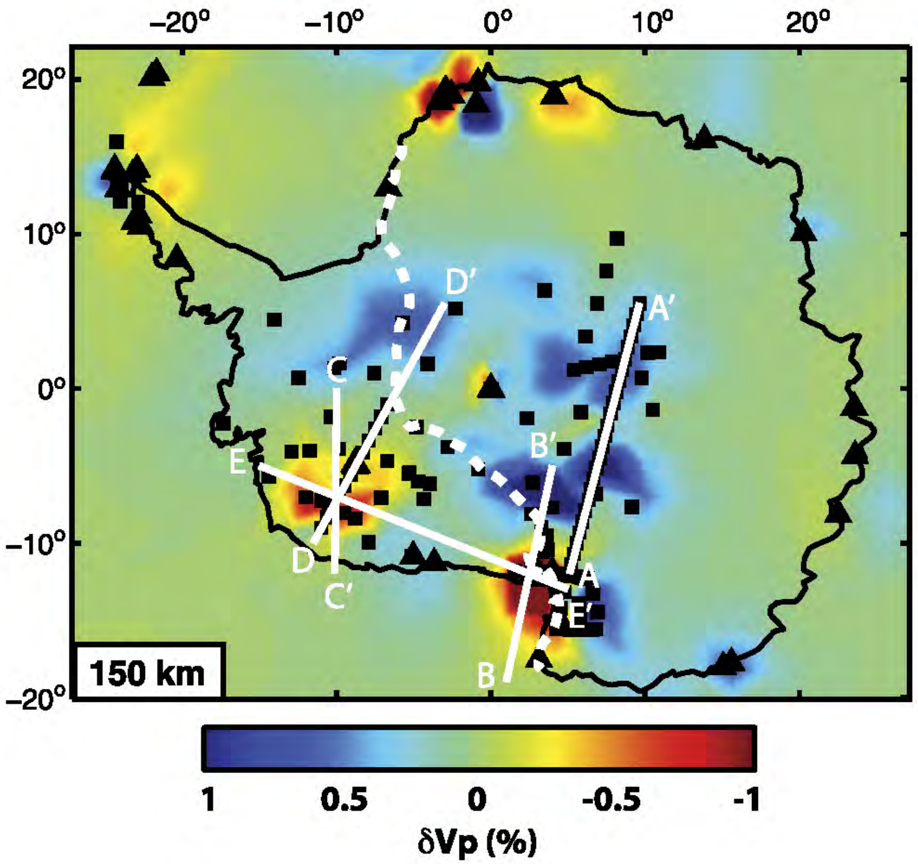

Hansen et al. (2014)

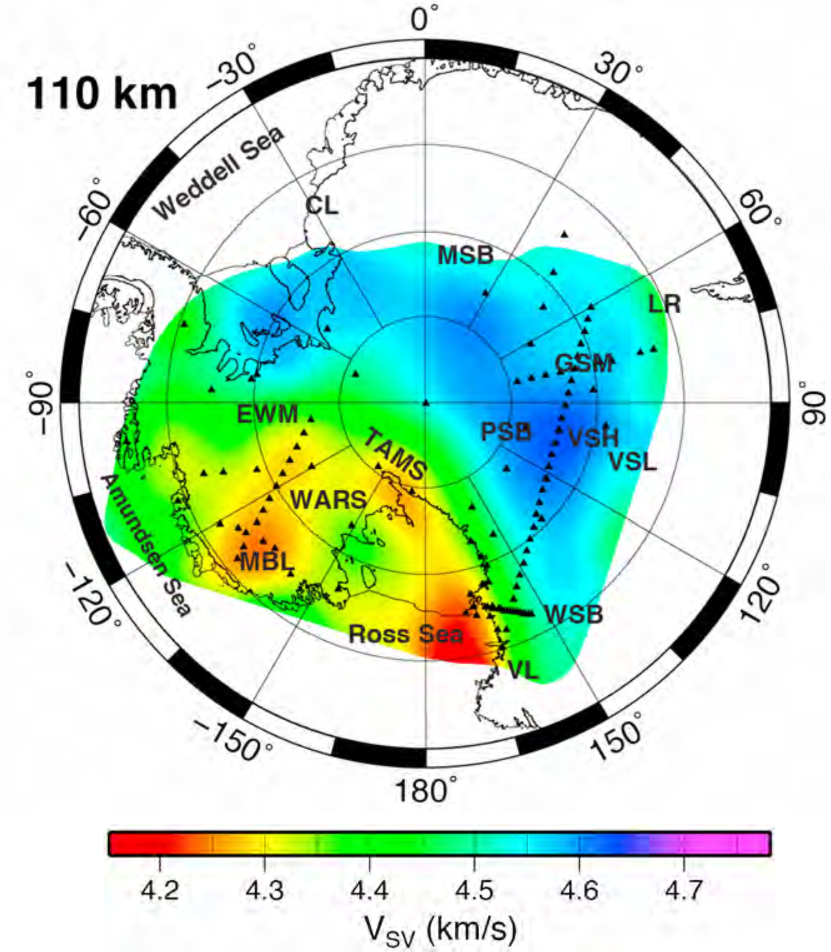

Heezel et al. (2016)

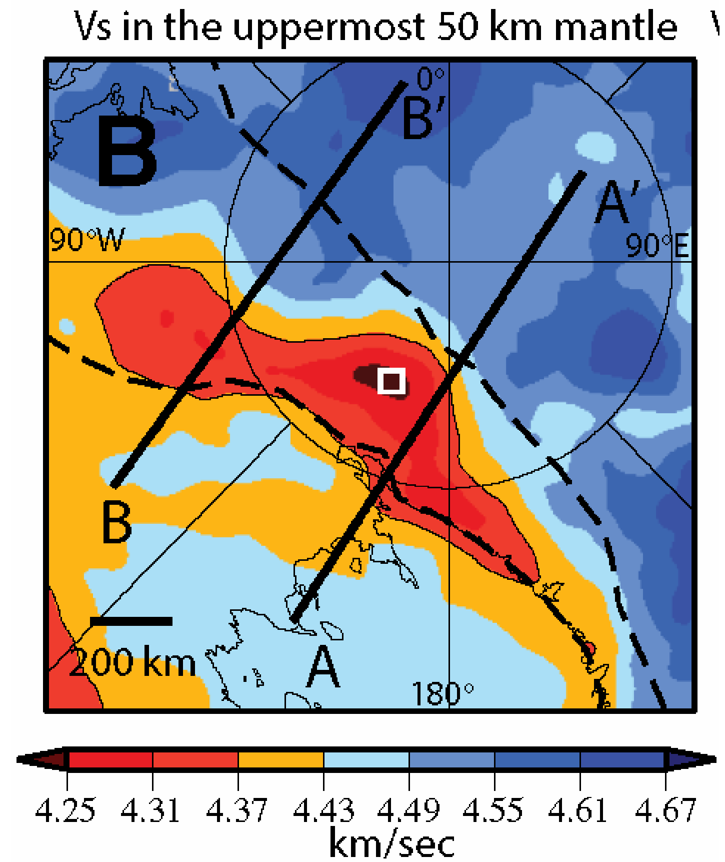

Shen et al. (2017)

Seismic tomography models from new arrays
(Polenet, Tamnnet, Tamseis, Gamseis)

Motivations:

- Rifting one of 3 main modes of mountain building, volcanism.
- General goal to examine well-expressed modes worldwide.
- Rift regimes contain resources, host earthquakes.
- Understand transition between stretching and stable margins.
- What supports high mountains?, what controls decay of elevation?
- Compare to well-known Great Basin margins.
- How do CO_2-dominated phonolitic rift volcanoes differ from H_2O-dominated subduction volcanoes?
- What are the differentiation and staging regions for phonolites?

Approaches:

- Must understand the third dimension (depth): geophysics.
- Seismology has had limited success: coverage, sources.
- Physical property of electrical conductivity reflects melt, fluids, hydration.
- Magnetotelluric (MT) method: broadband global EM source.
- Need to adapt traditional land method to polar ice sheets.

Source Fields for the Magnetotelluric Method

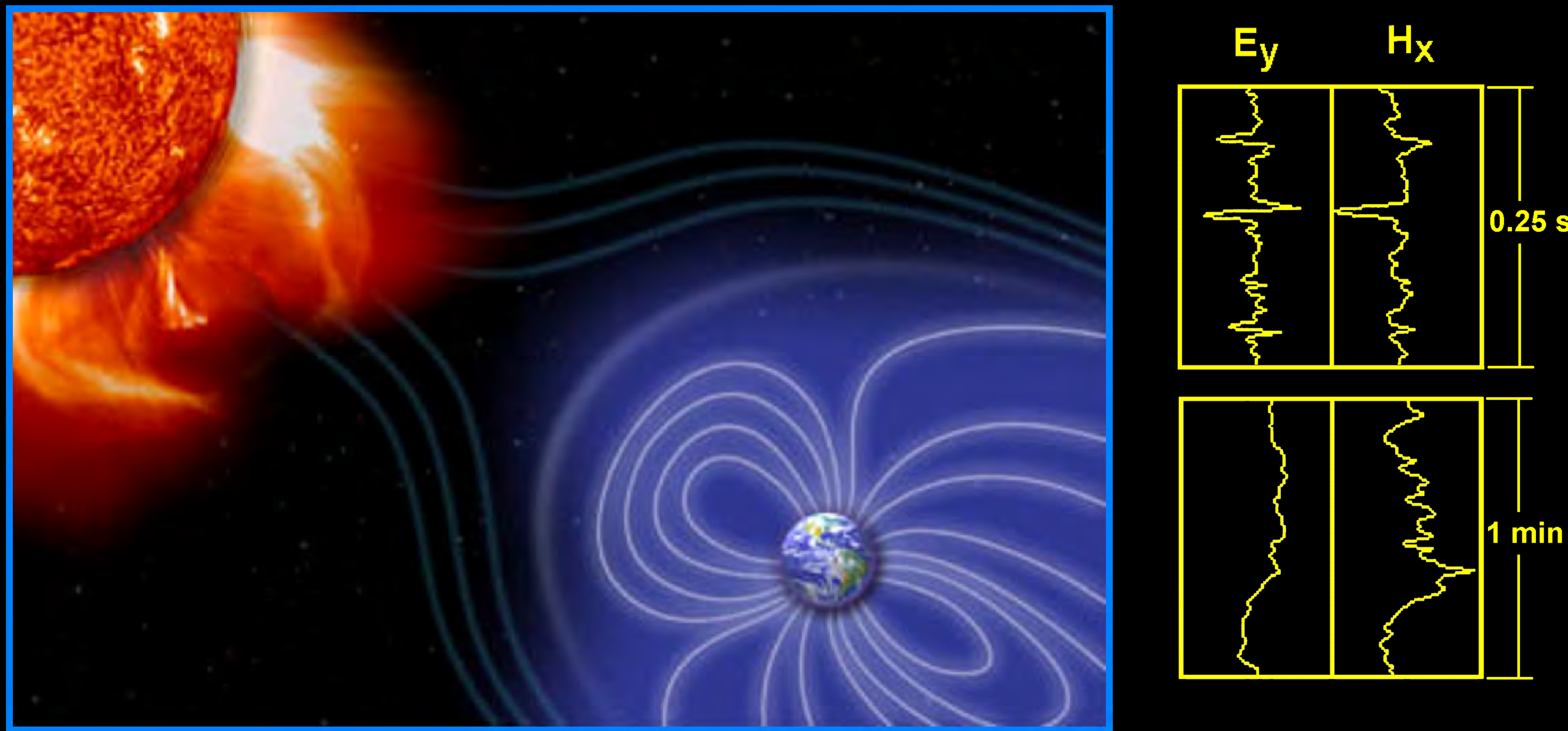

Regional and Global Lightning Activity for f > 1 Hz
Solar Wind-Magnetospheric Interactions for f < 1 Hz

MT Recording Components For Polar Deployment

Induction Coil (Solenoid)

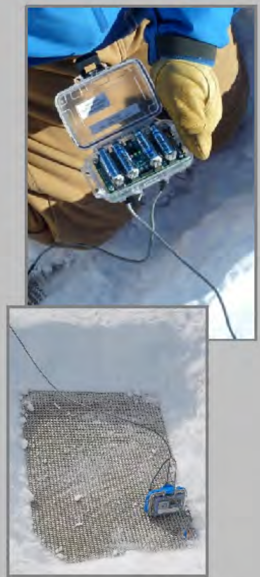

Ti Electrode w/ High-Z Preamp

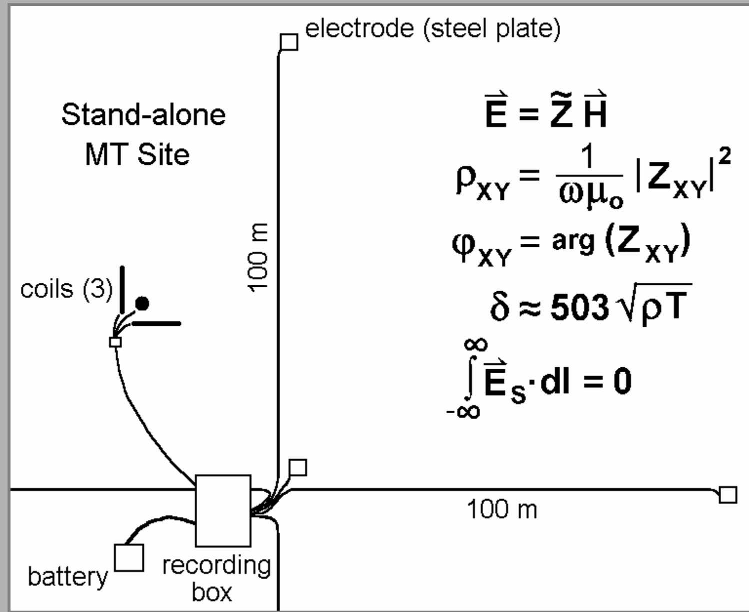

$$\vec{E} = \tilde{Z}\,\vec{H}$$

$$\rho_{XY} = \frac{1}{\omega\mu_o}\,|Z_{XY}|^2$$

$$\varphi_{XY} = \arg(Z_{XY})$$

$$\delta \approx 503\sqrt{\rho T}$$

$$\int_{-\infty}^{\infty} \vec{E}_S \cdot dl = 0$$

Sync'd MT recorders

MT Recording Components For Polar Deployment

Induction Coil (Solenoid)

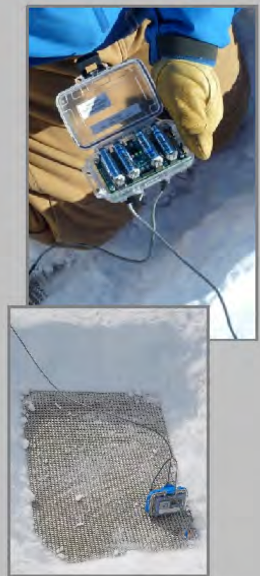

Ti Electrode w/ High-Z Preamp

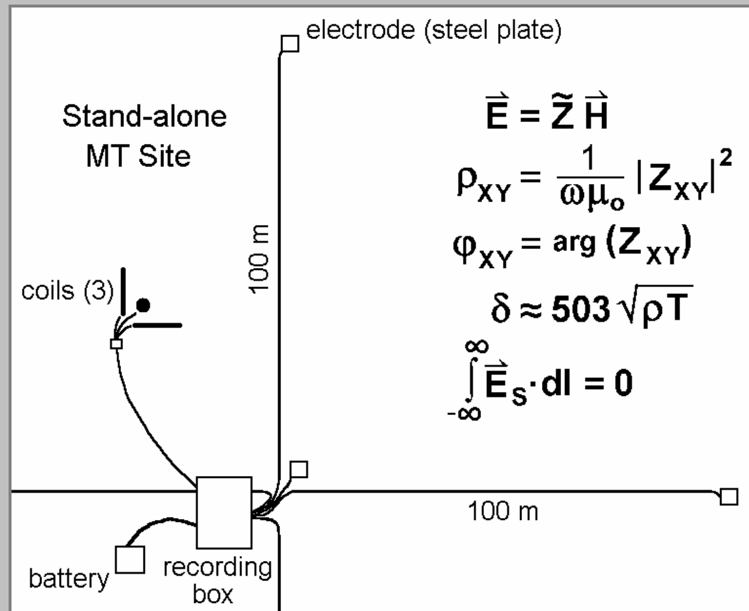

Sync'd MT recorders

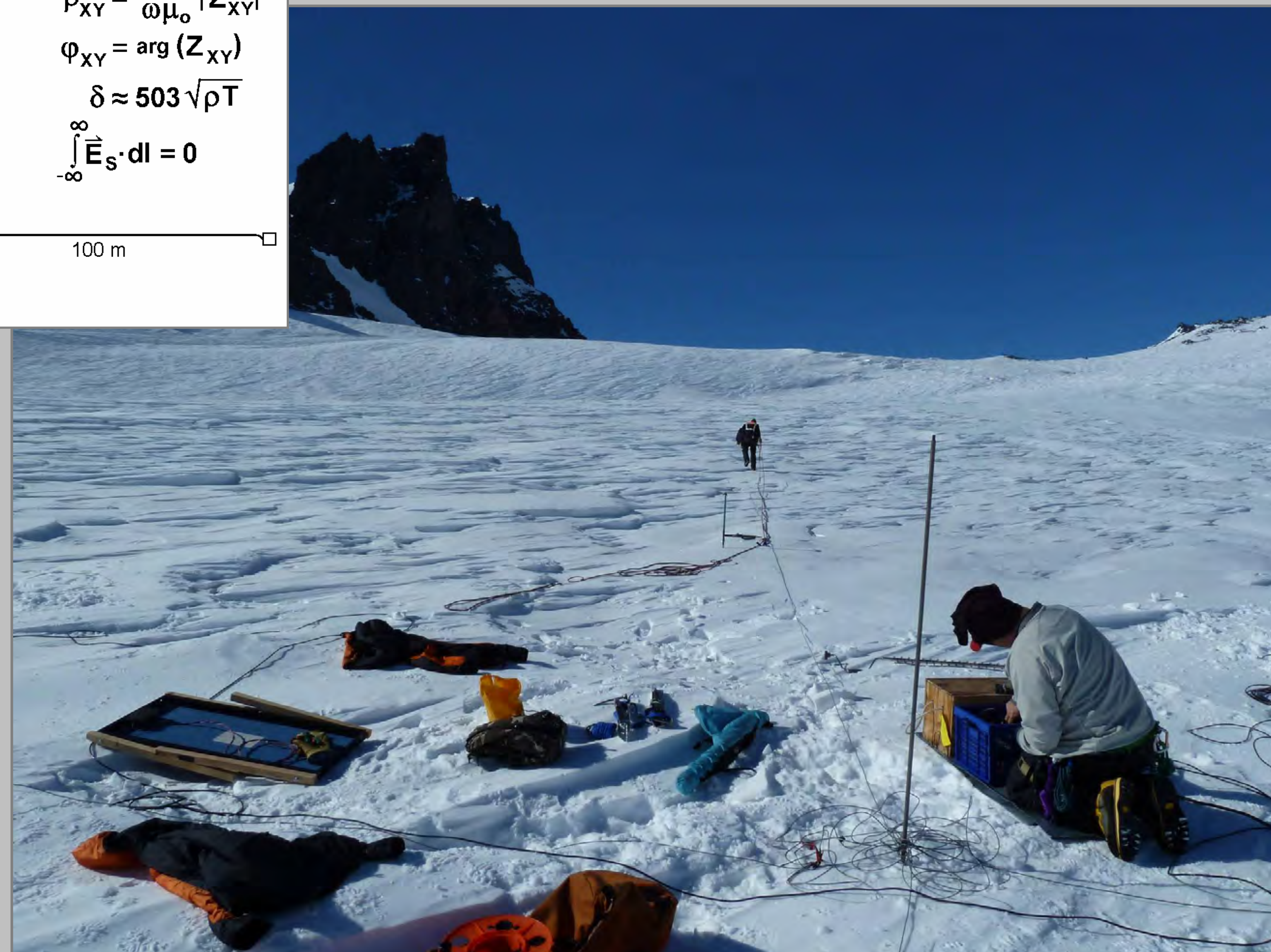

MT Recording Components For Polar Deployment

Induction Coil (Solenoid)

Ti Electrode w/ High-Z Preamp

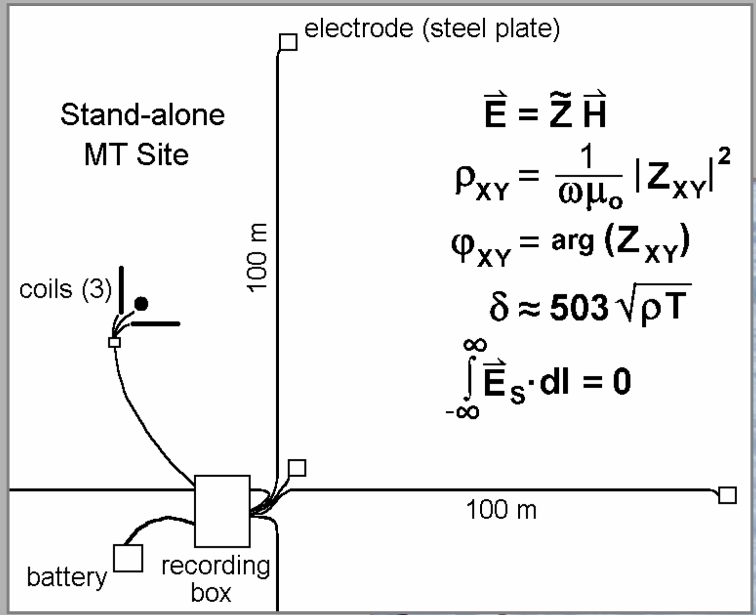

Sync'd MT recorders

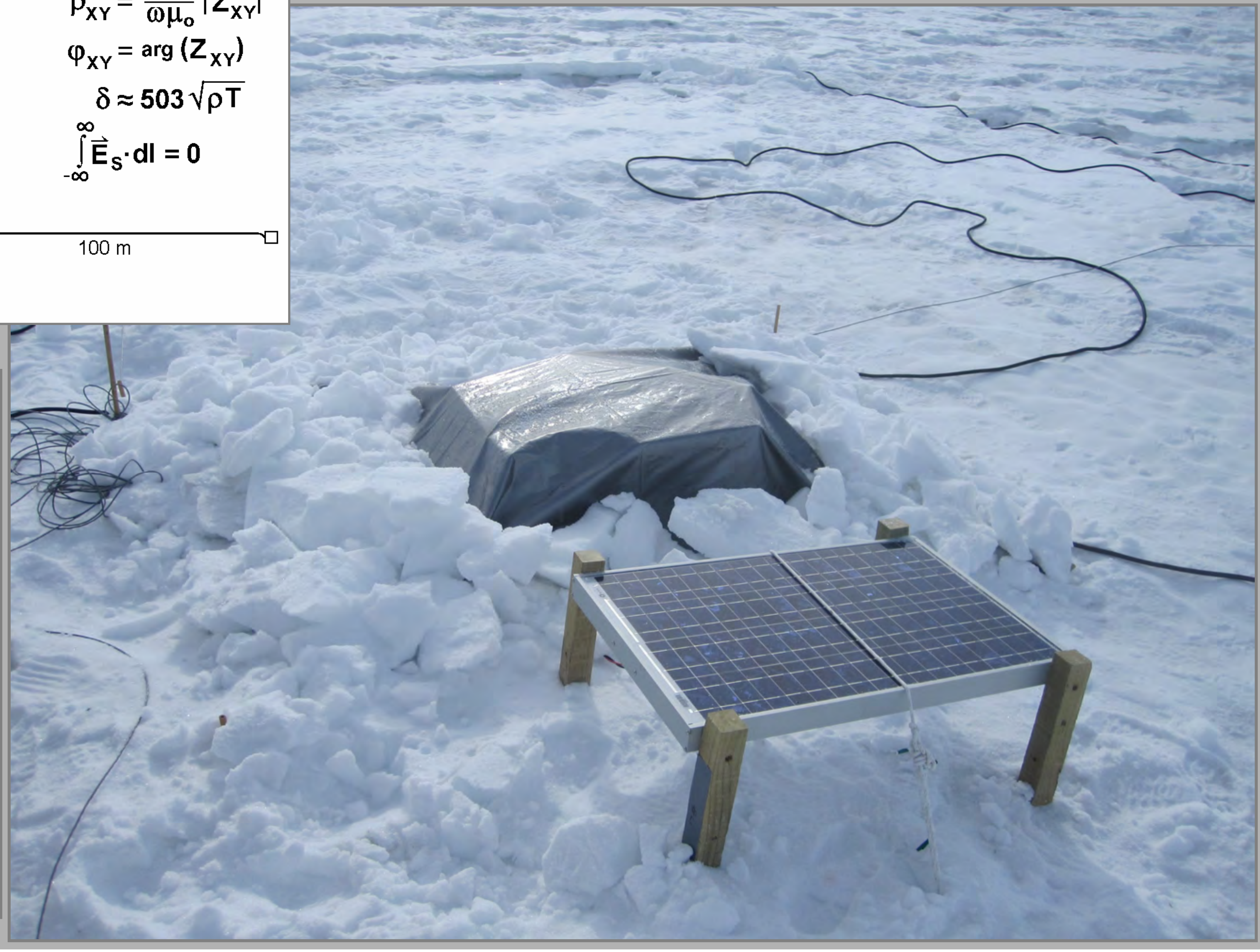

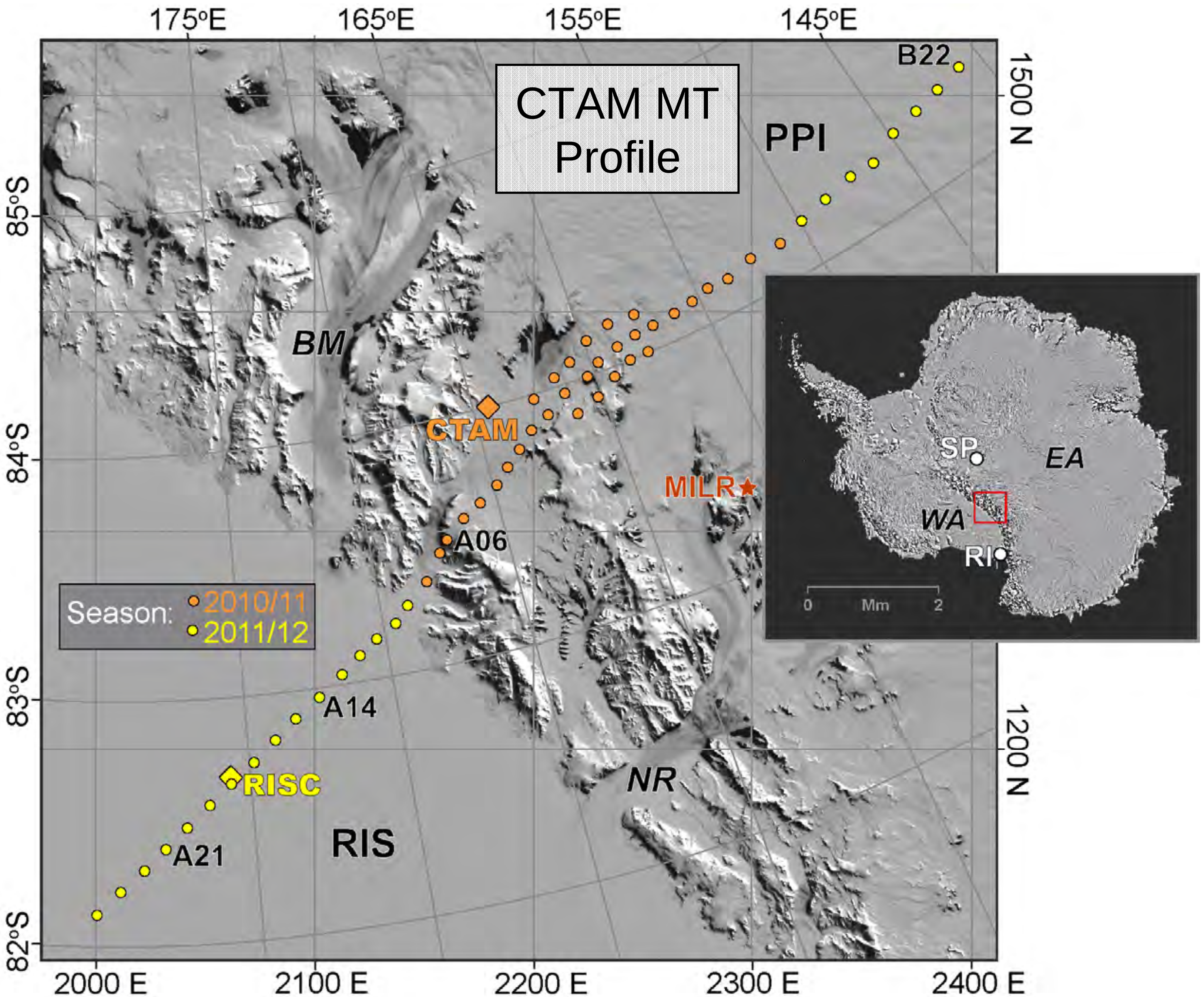

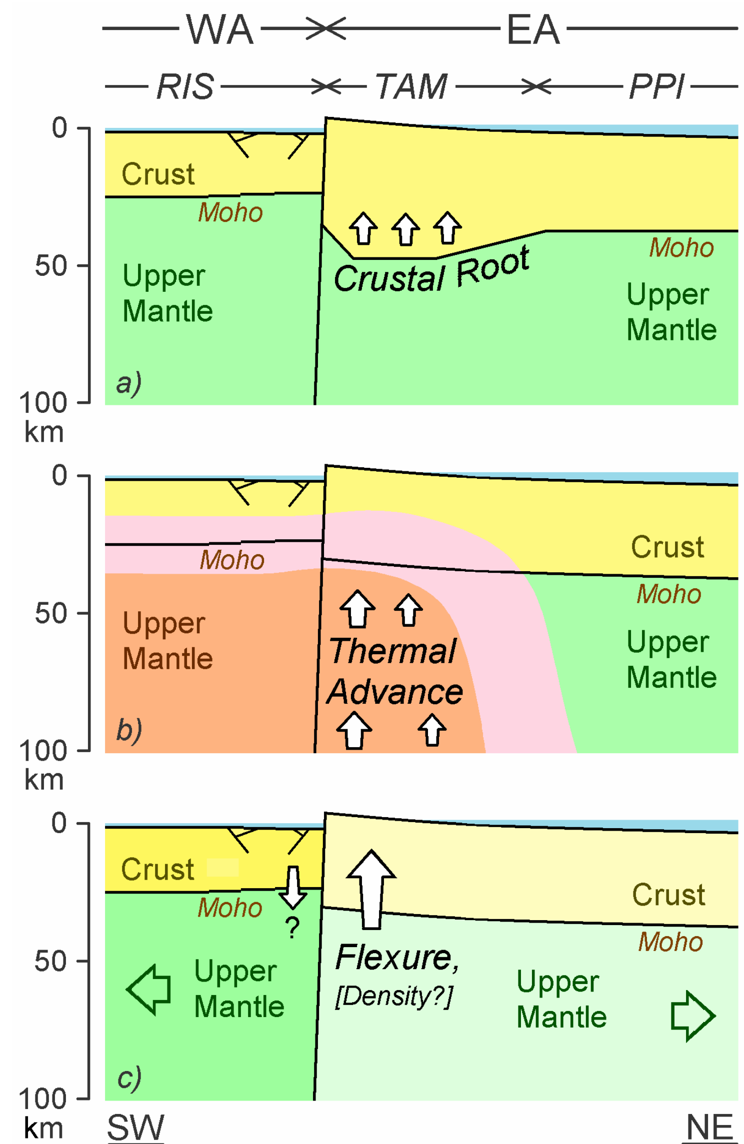

Hypotheses for TAM Uplift

(Wannamaker et al., 2017, Nat Comms)

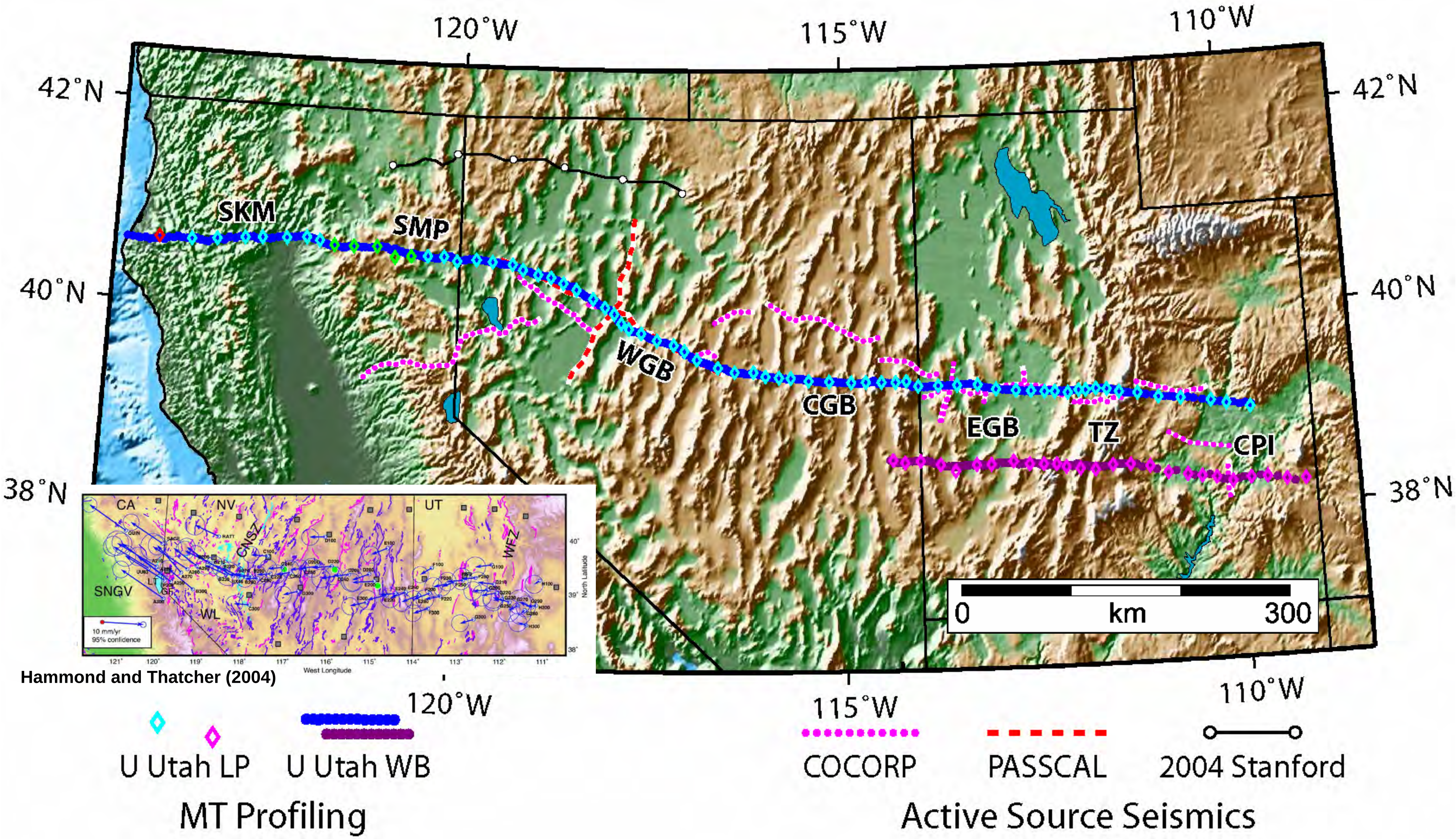

S Klamath Mtns – Great Basin – Colorado Plateau MT

Approx. coincident with COCORP, PASSCAL seismic profiling

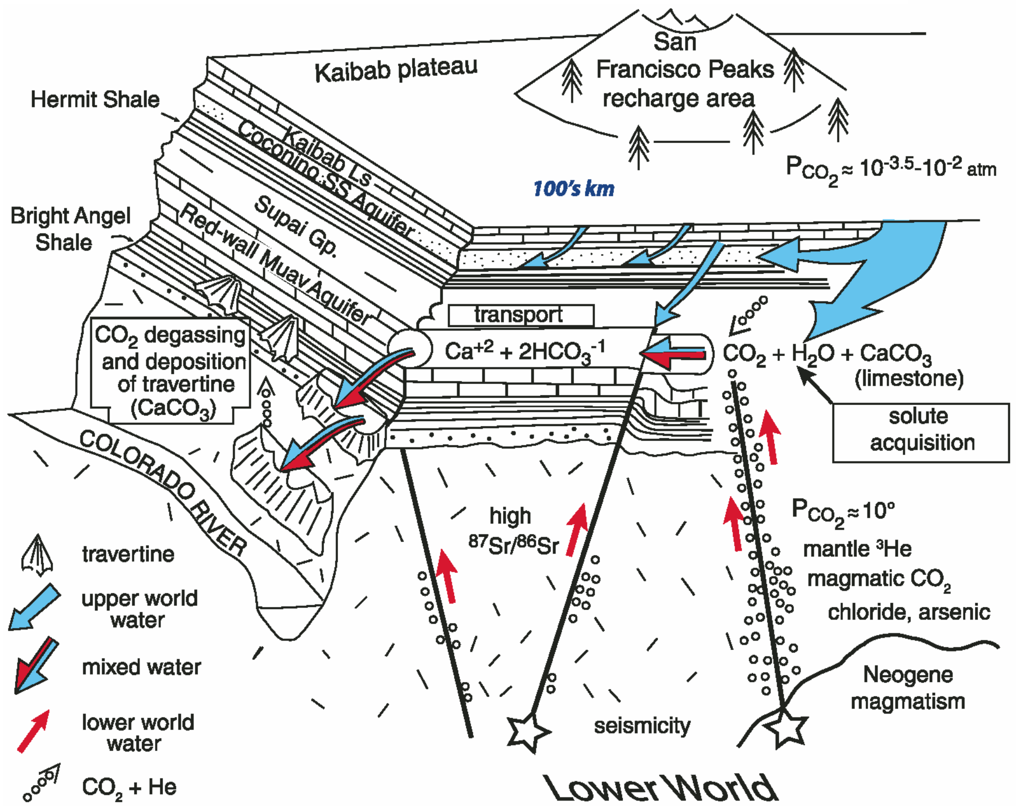

Multiscale Magmatic/ Hydrothermal Connections

Grand Canyon Hydrol. Model
(Crossey and Karlstrom, 2012)

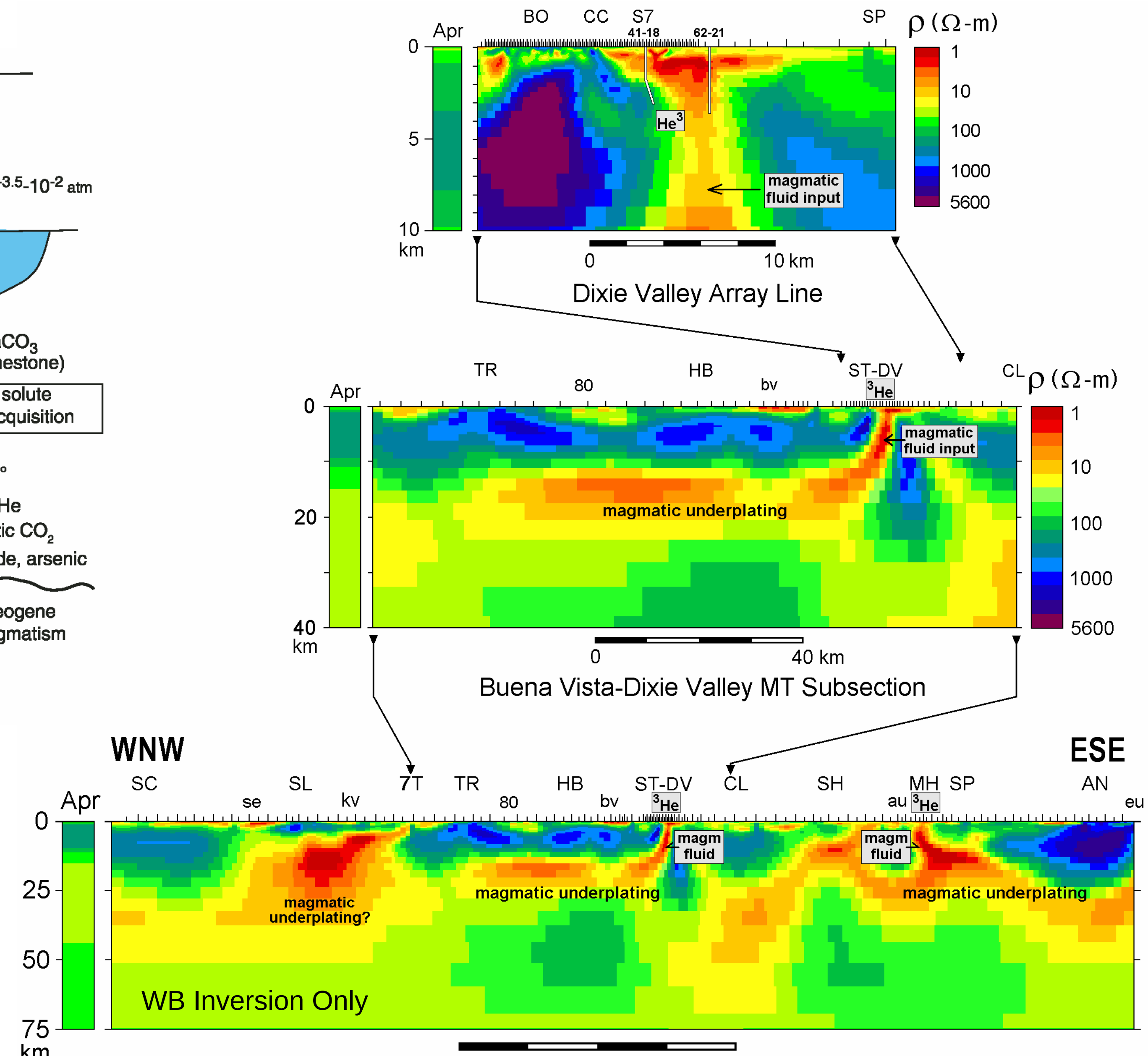

NW Great Basin MT Transect

Wannamaker et al, 2007, 2008, 2011; Siler et al., 2014

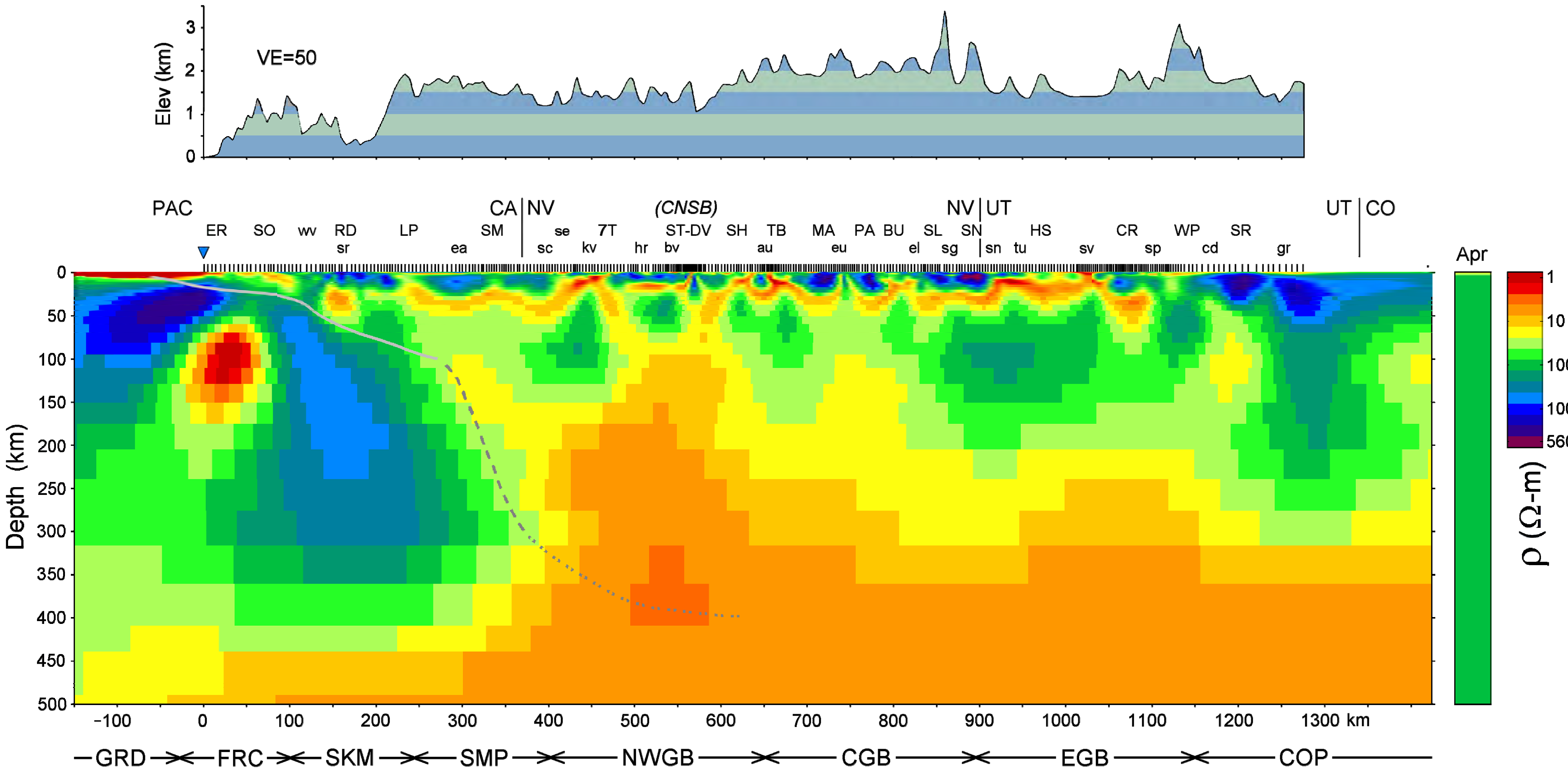

Klamath - S Modoc - Great Basin - Colorado Plateau

MT Transect (~40 N lat.)

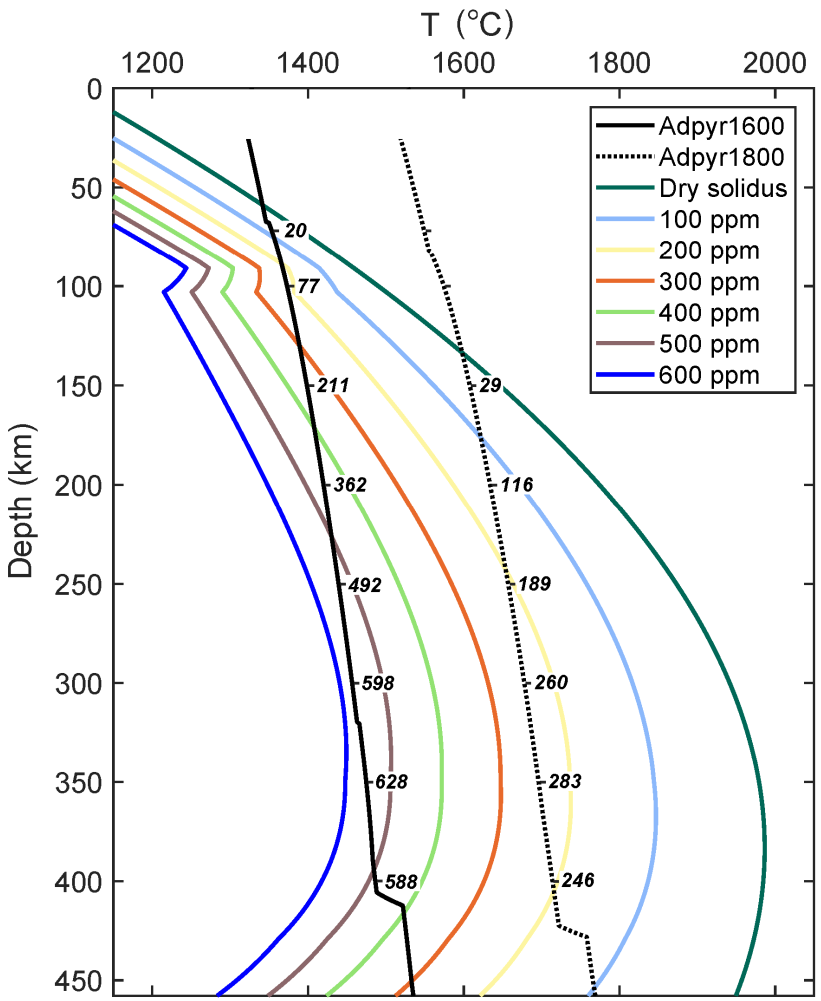

Hirschmann et al (2009, PEPI)
Stixrude and Lithgow-Bertelloni (2011, GJI)

Novella et al (2014, EPSL)

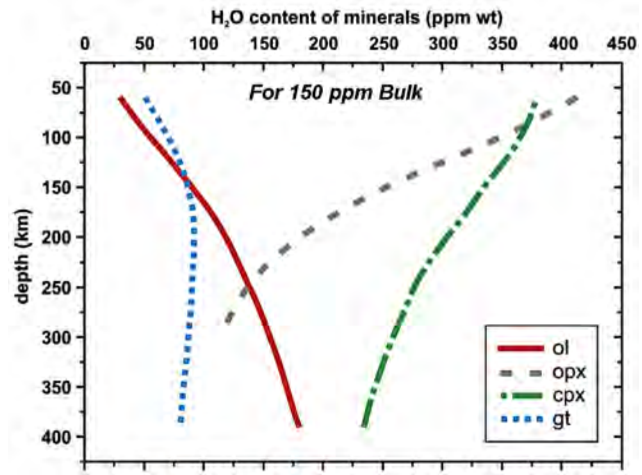

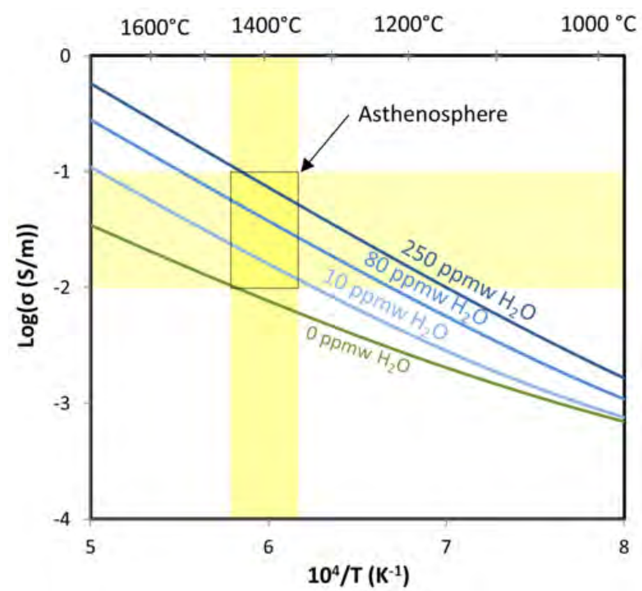

Novella et al (2017, Sci Rpt)

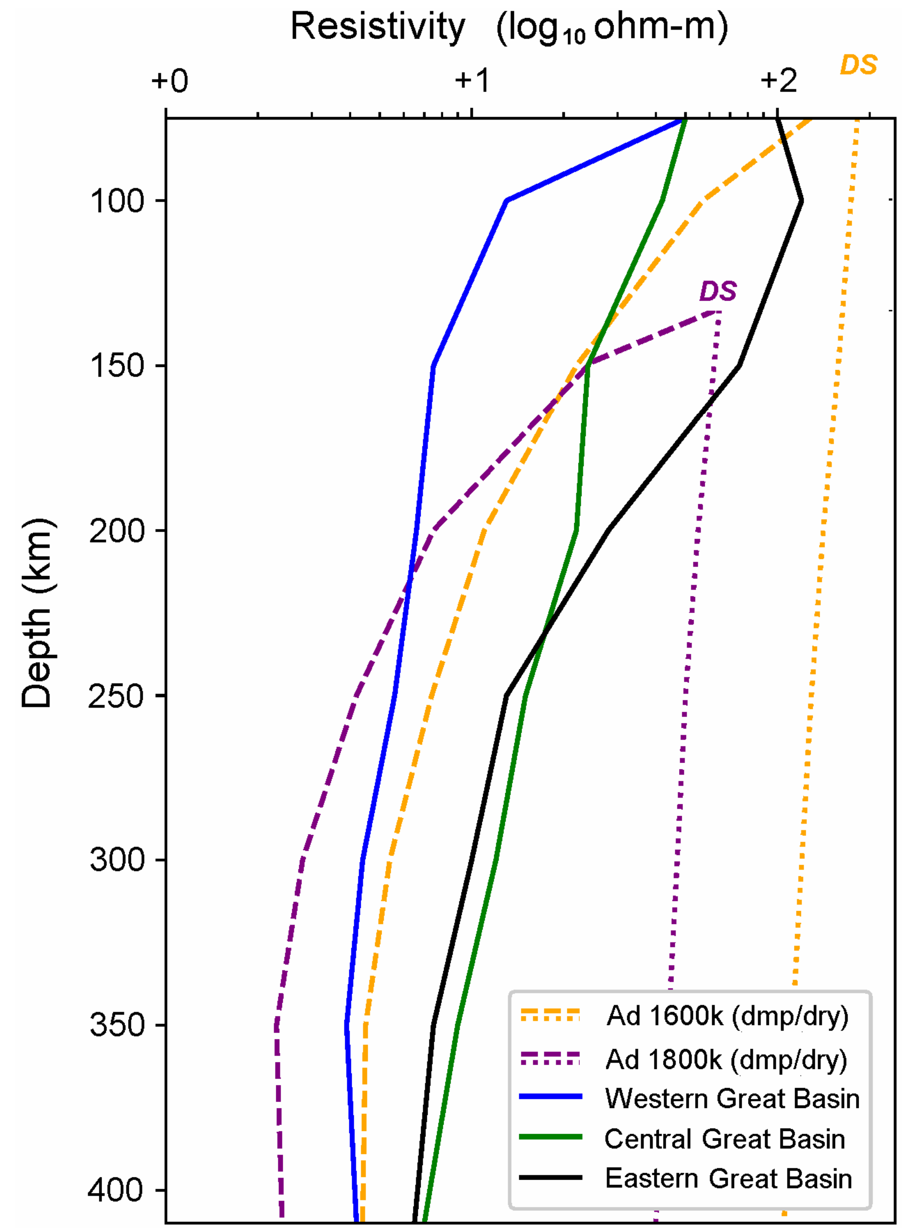

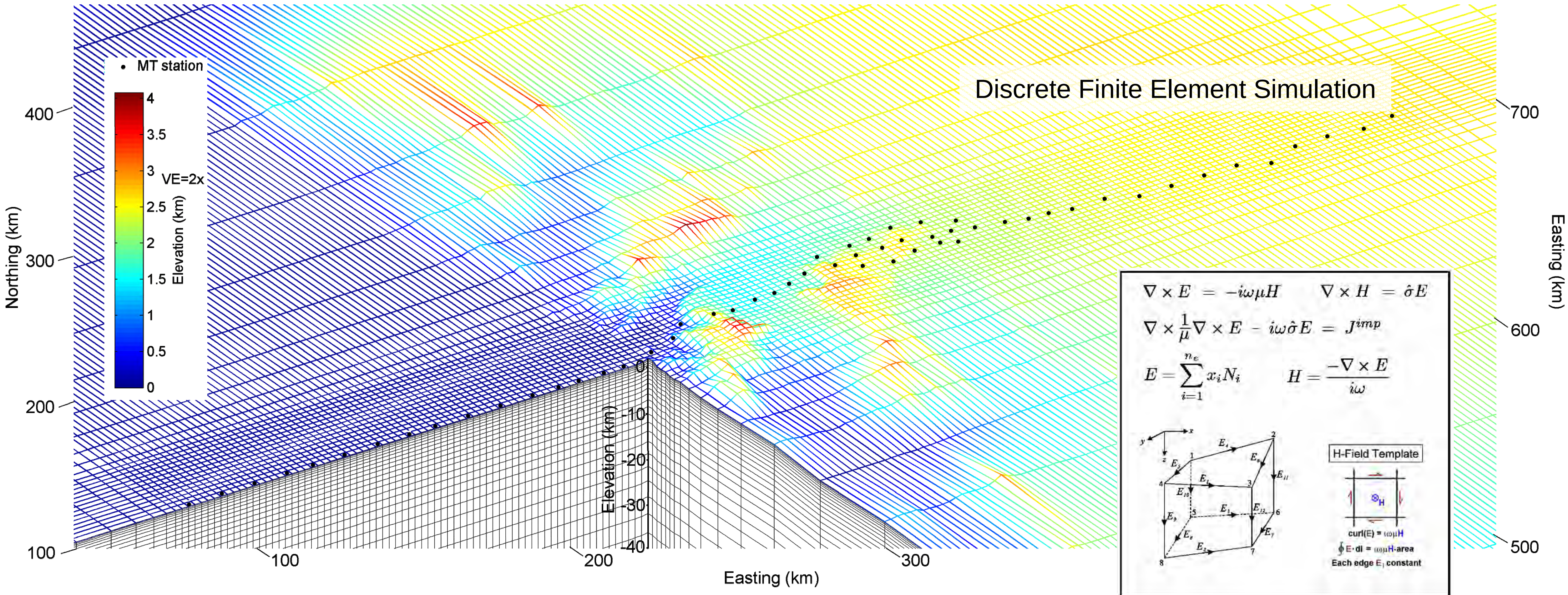

EM Field (Maxwell) Equations
And Deformed Finite Element

Objective: $W_\lambda(m) = \{(d - F[m])^T C_d^{-1}(d - F[m])\} + \lambda\{(m - m_o)^T C_m^{-1}(m - m_o)\}$

NL Step: $m_{k+1} - m_k = \{J_k^T C_d^{-1} J_k + \lambda C_m^{-1}\}^{-1}\{J_k^T C_d^{-1}(d_k - F[m_k]) - \lambda C_m^{-1}(m_k - m_o)\}$

Stabilized Iterative Earth Resistivity Voxel Estimation (Tarantola, 1987)
NL Step Recast to Data-Space Formulation (Parker, 1994)

Can Invert for Impedance Static Distortions (Avdeeva et al., 2015)
Direct Matrix Solutions Used Throughout (Metis, Pardiso, Plasma)
Parallelized on Large RAM, Single-Box Workstations

3D MT Inversion of Using Deformable Edge Finite Element Algorithm (Kordy, Wannamaker, et al., 2016, GJI)

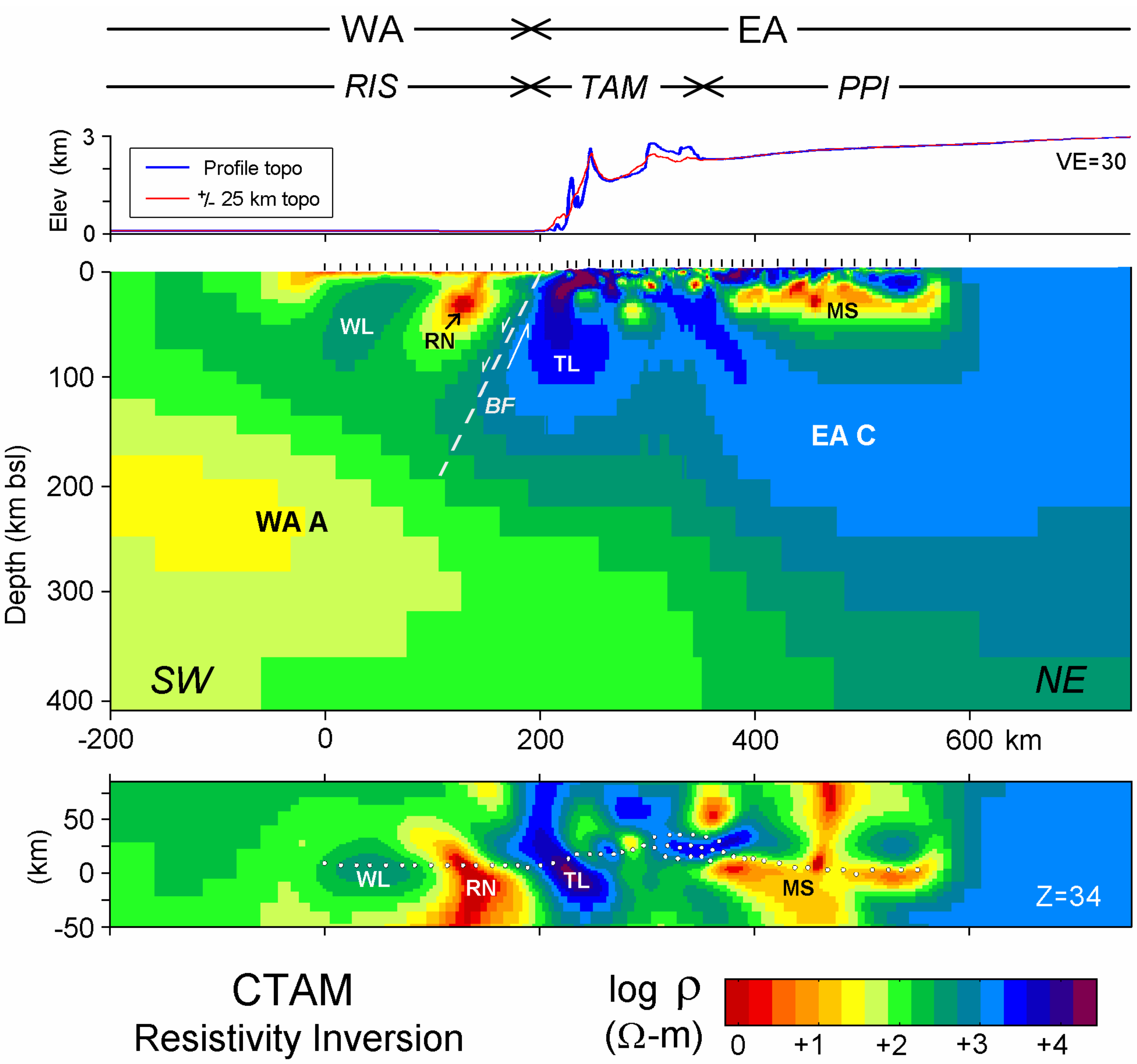

CTAM
Resistivity Inversion

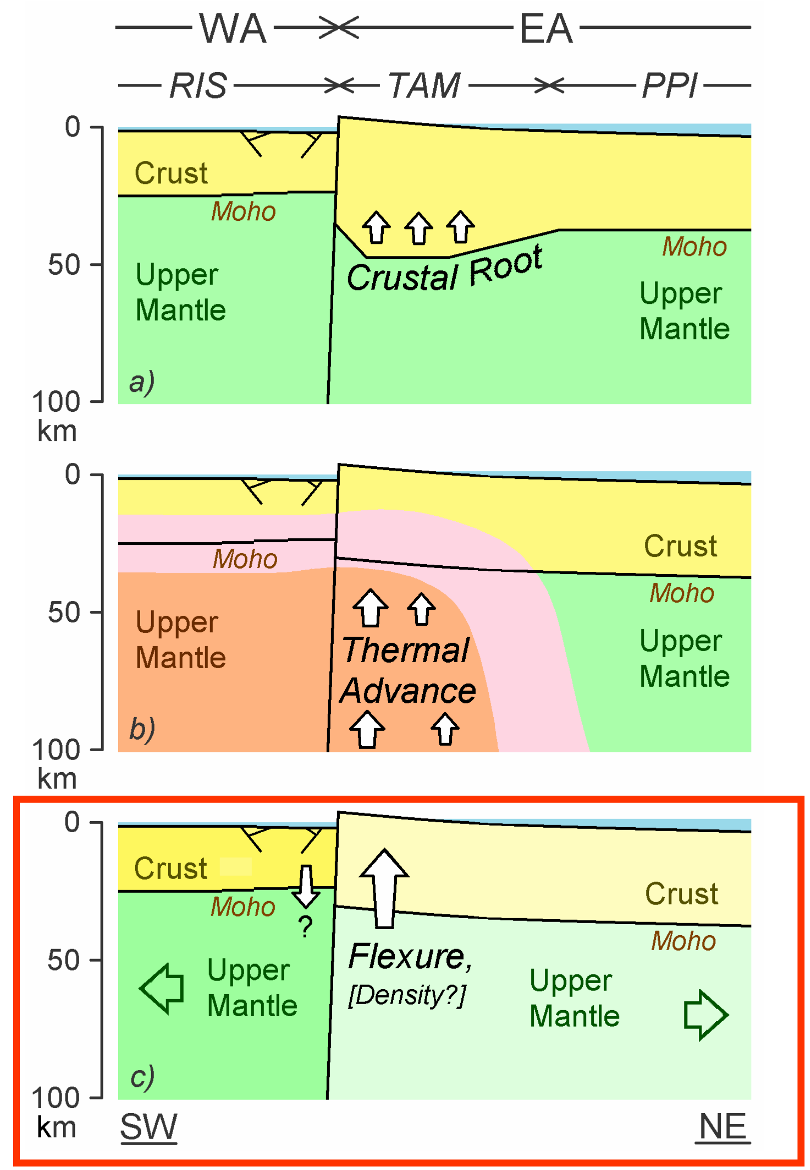

Hypotheses for TAM Uplift

(Wannamaker et al., 2017, Nat Comms)

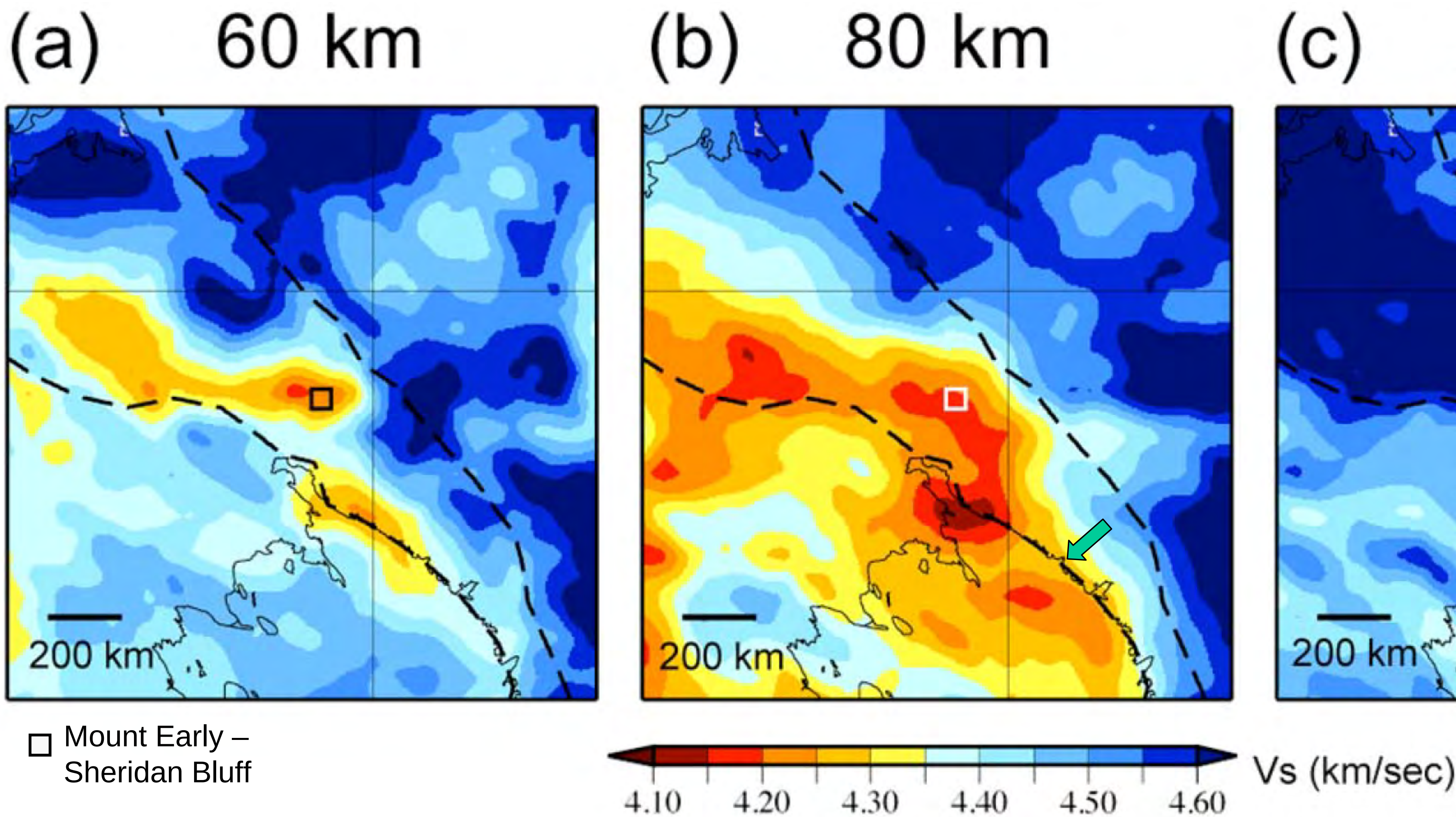

Absolute Shear Wave Speeds
Southern Transantarctic Mountains
(Shen et al., 2017)

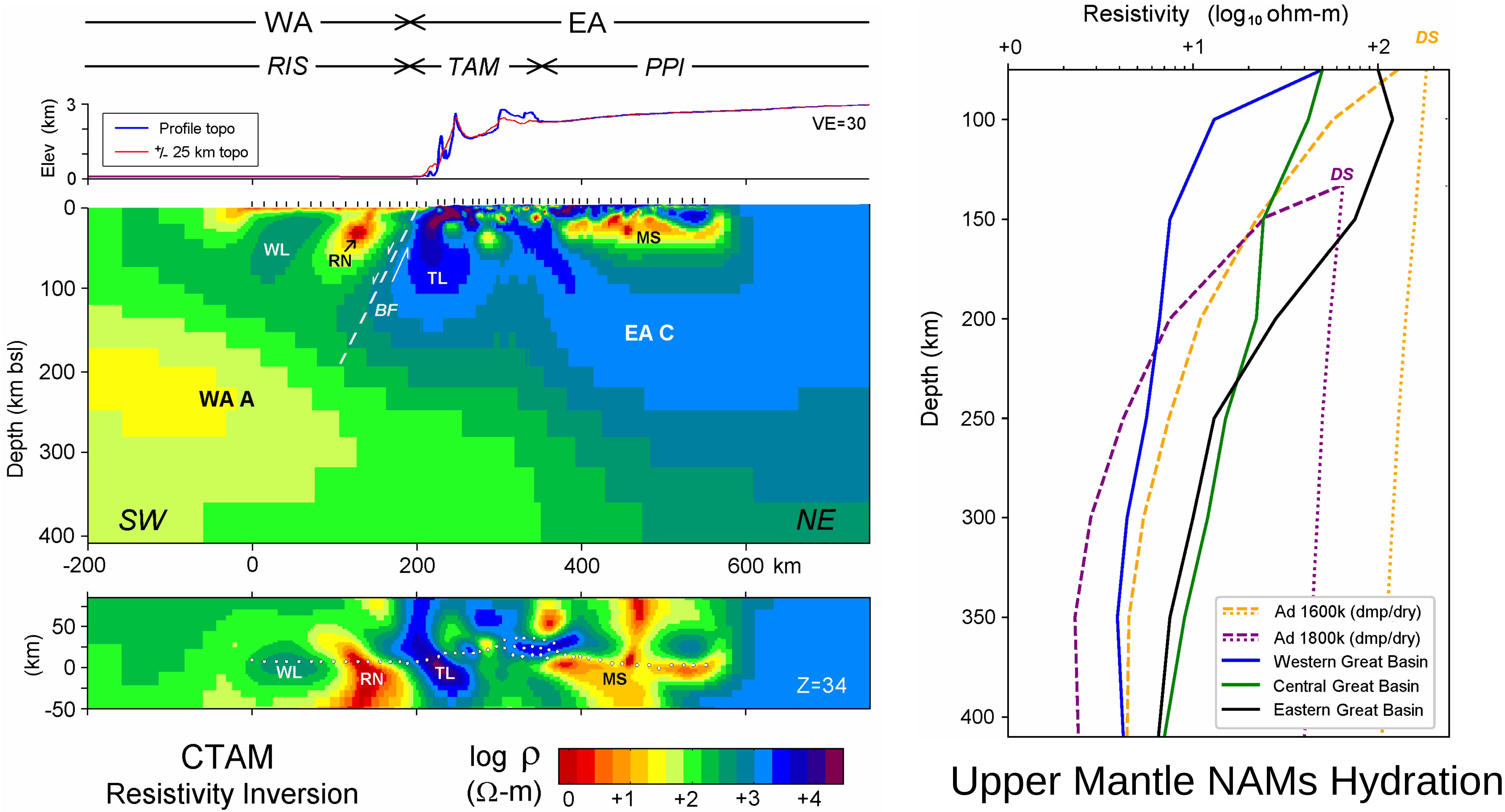

WA
EA
RIS
TAM
PPI
Elev (km)
Profile topo
+/- 25 km topo
VE=30
Depth (km bsl)
WL
RN
TL
BF
MS
EA C
WA A
SW
NE
-200
0
200
400
600 km
(km)
Z=34
CTAM
Resistivity Inversion
log ρ
(Ω-m)
0
+1
+2
+3
+4
Resistivity (log10 ohm-m)
+0
+1
+2
DS
Depth (km)
Ad 1600k (dmp/dry)
Ad 1800k (dmp/dry)
Western Great Basin
Central Great Basin
Eastern Great Basin
Upper Mantle NAMs Hydration

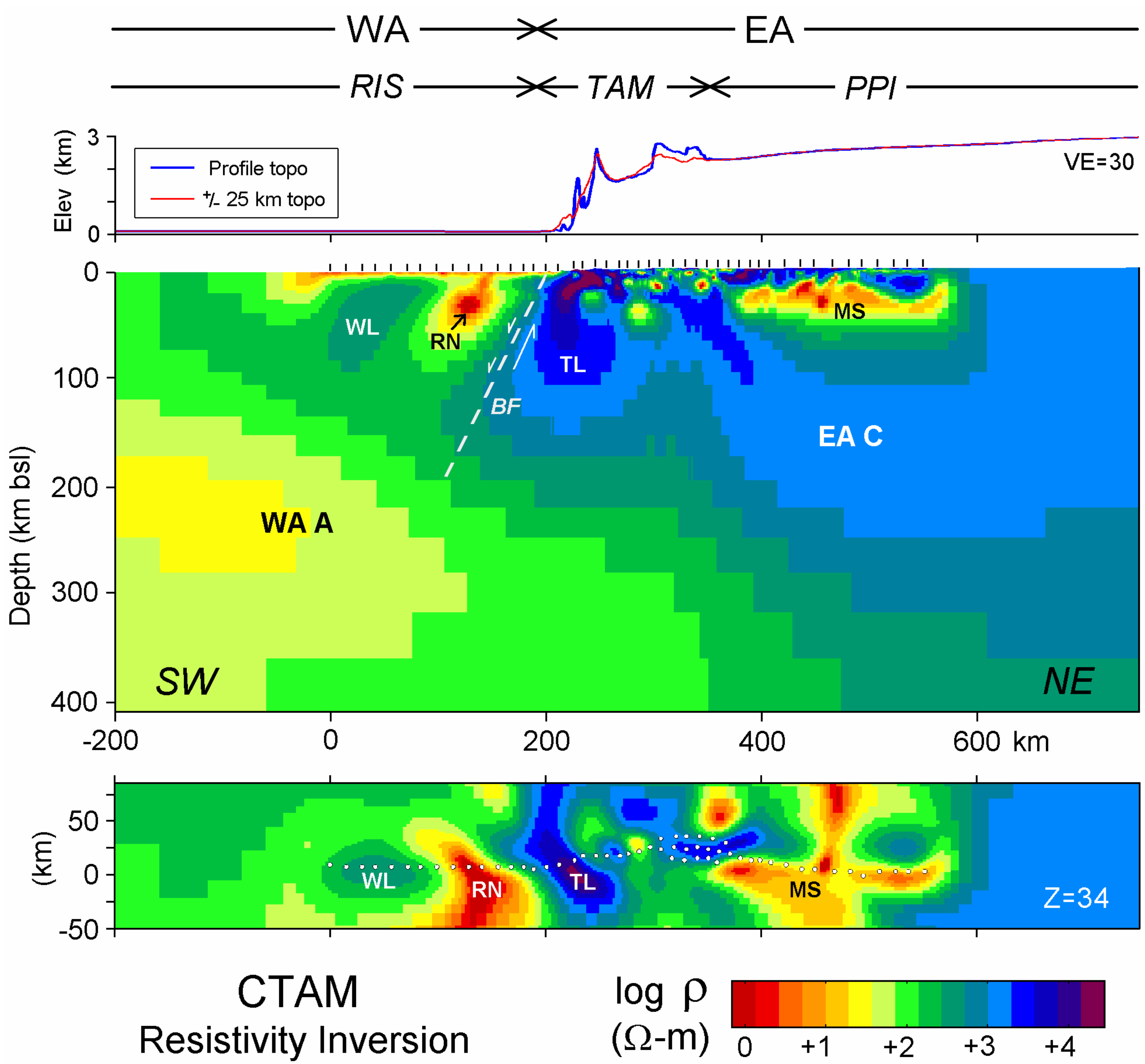

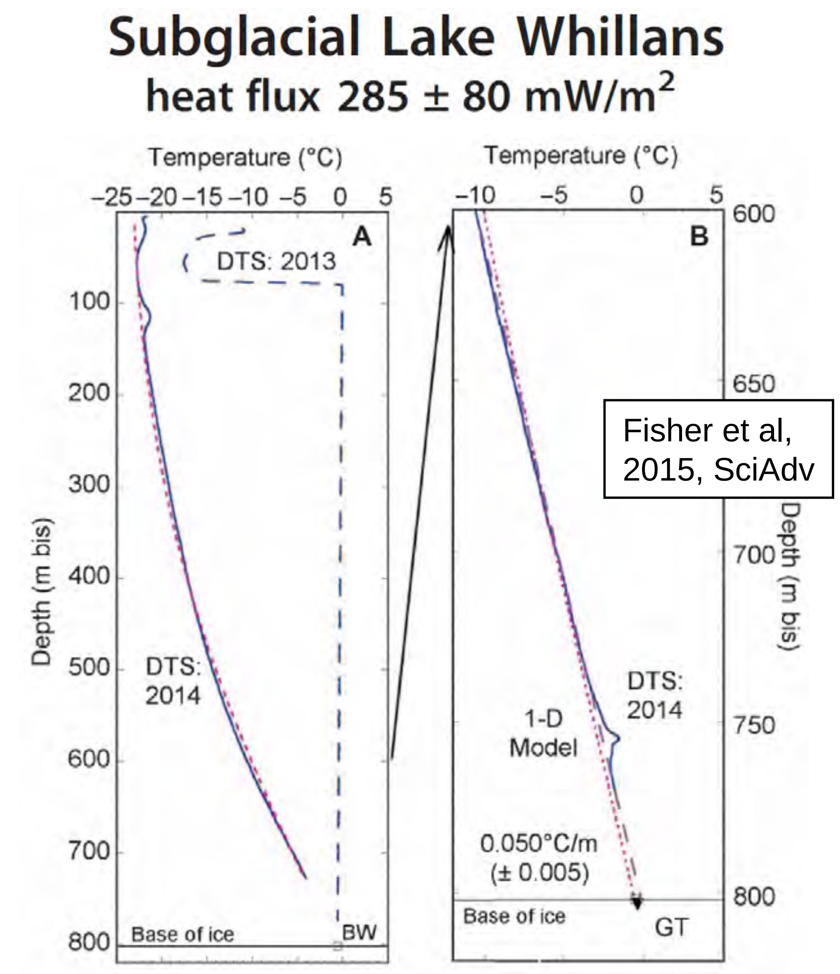

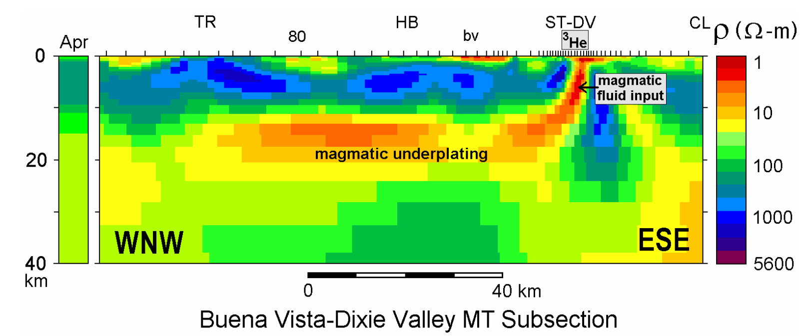

Rift Necking and Thermal Focus

Electrical conductivity and Paleo-Proterozoic foredeeps

D.E. Boerner, R.D. Kurtz, and J.A. Craven

JOURNAL OF GEOPHYSICAL RESEARCH, VOL. 101, NO. B6, 1996

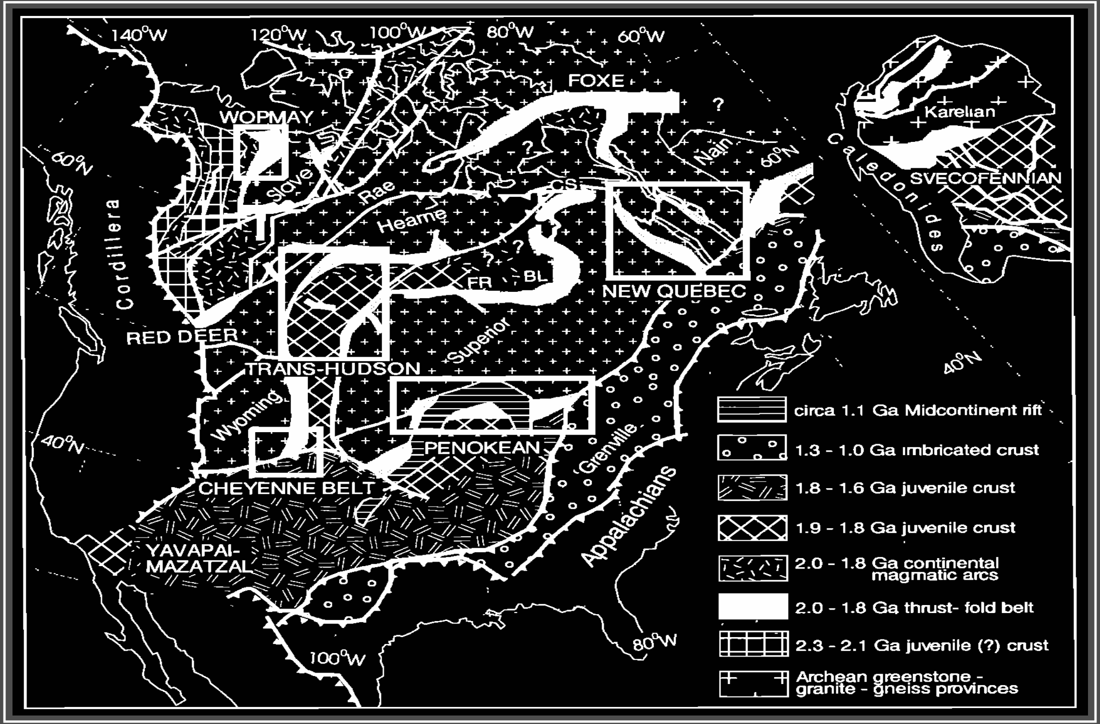

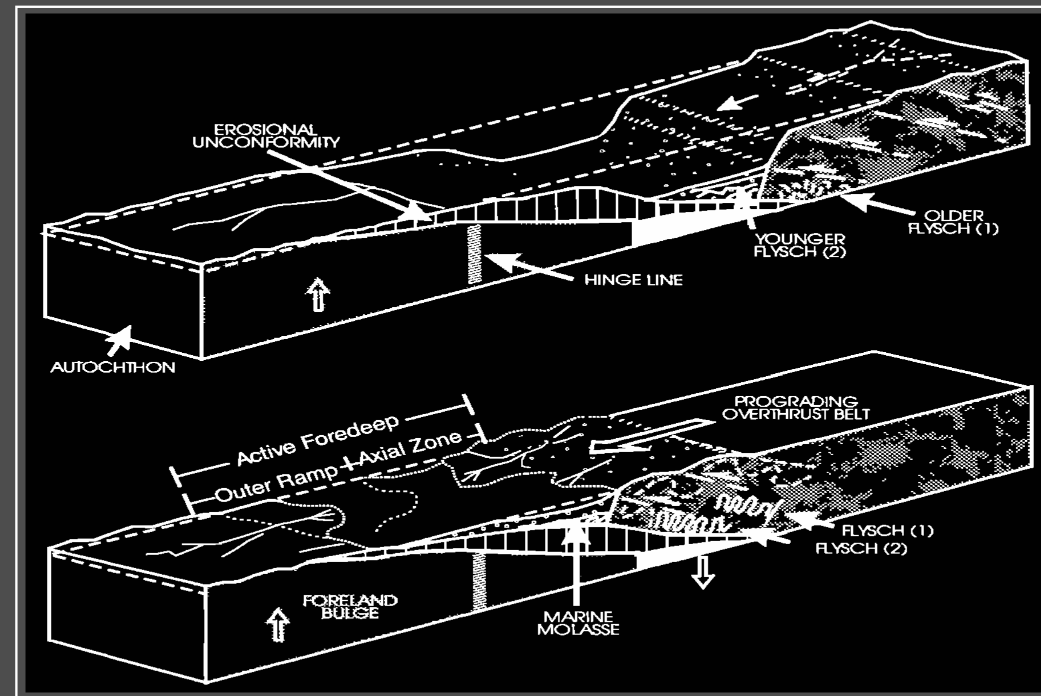

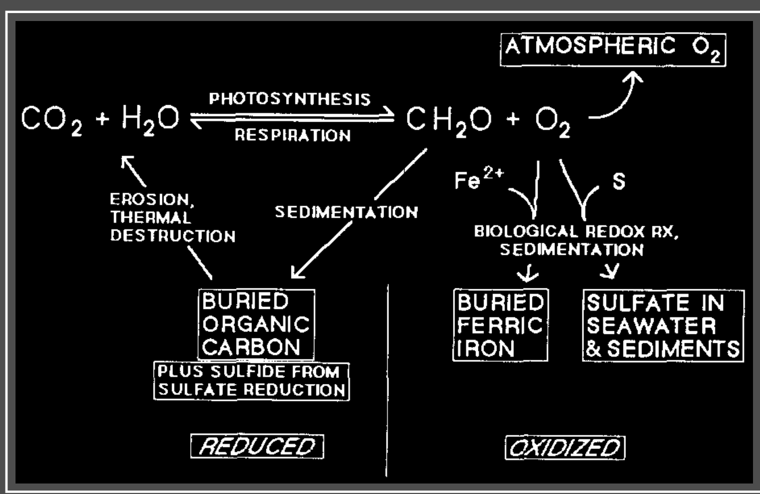

Cyanobacterial O production
← and oC-Sd sequestration
Des Marais (1994)

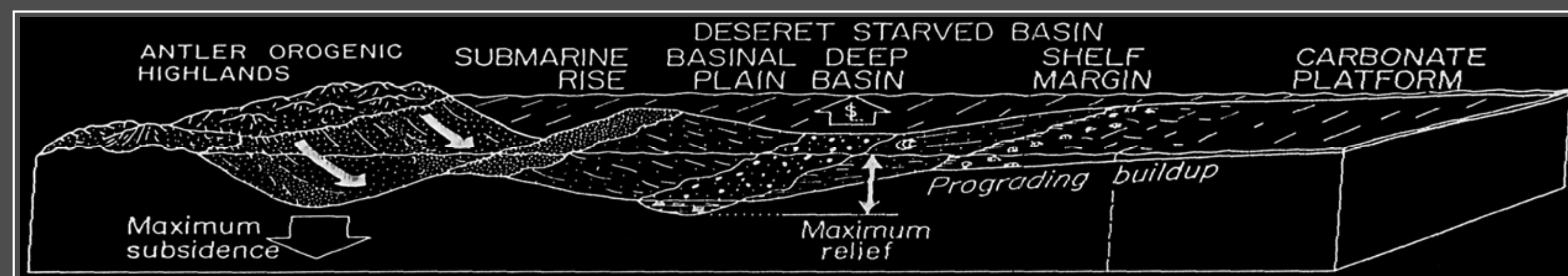

C-S concentration in starved basins
Sandberg and Gutschick (1983)

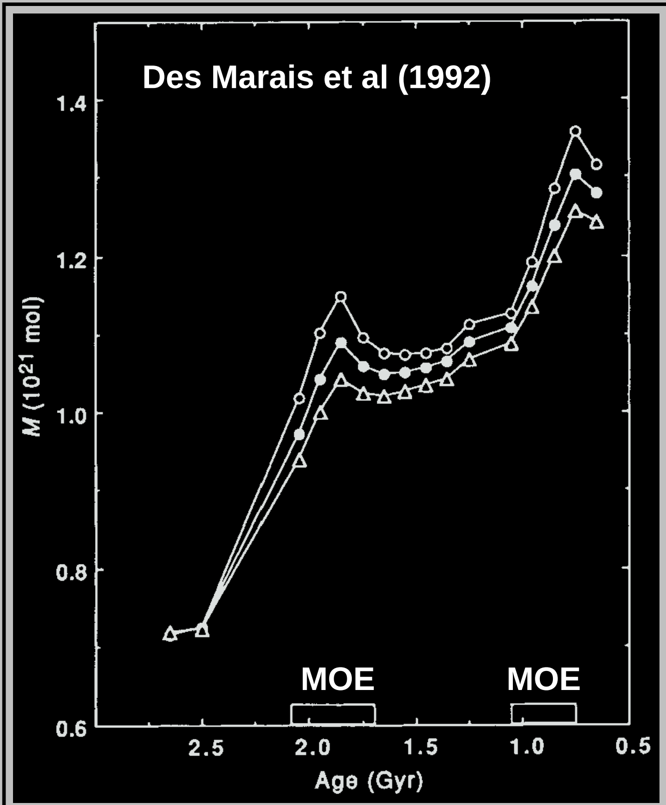

oC-Sd global primary production

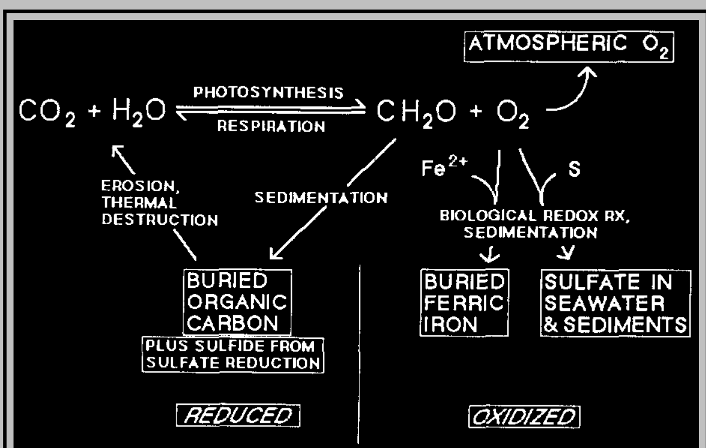

oC-Sd sequestration

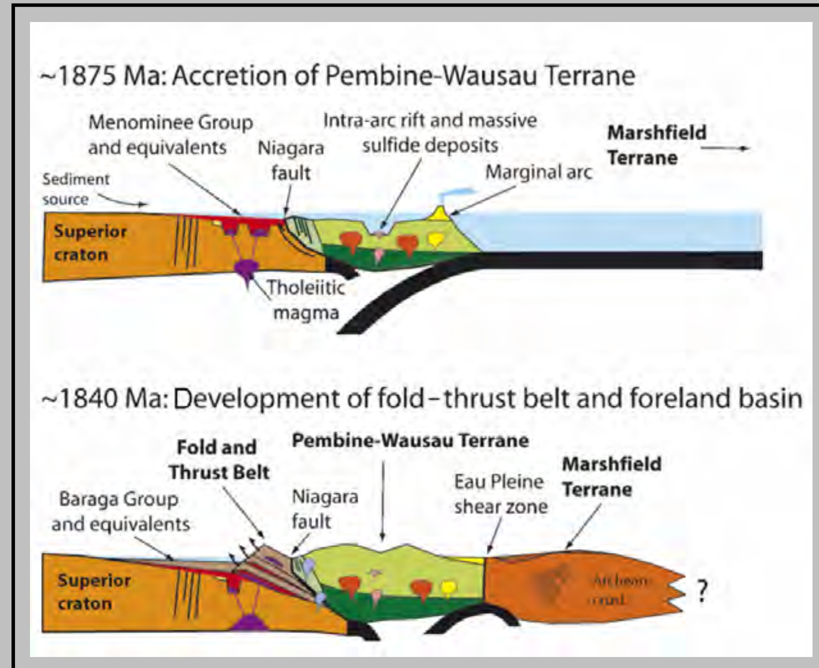

Mod from Schulz and Cannon (2007)

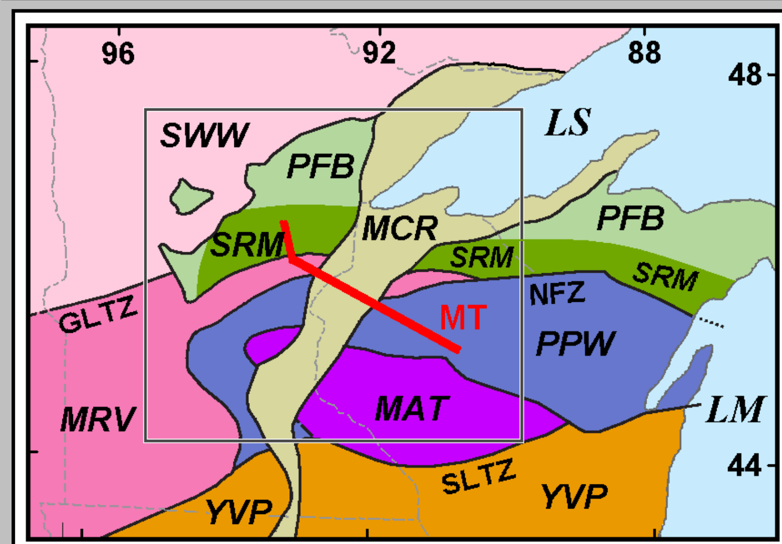

Mod from Southwick (2014)

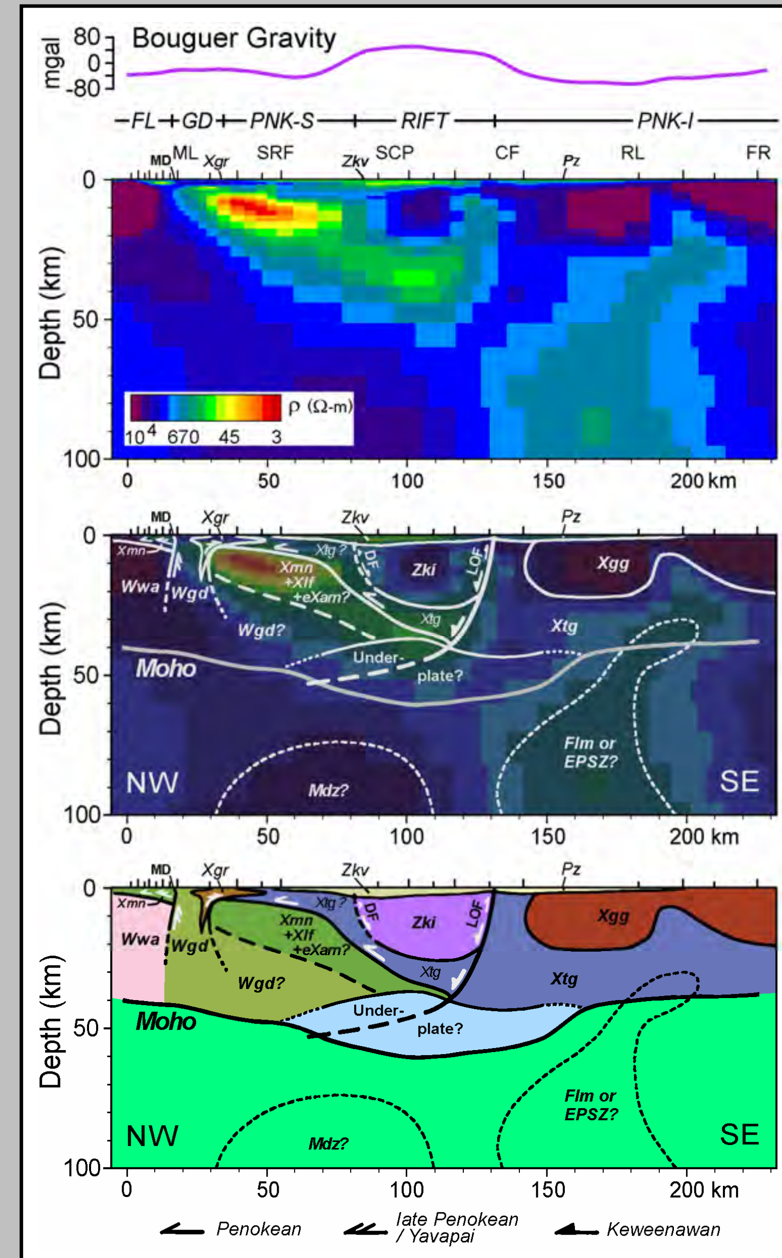

Wunderman et al. (2018)

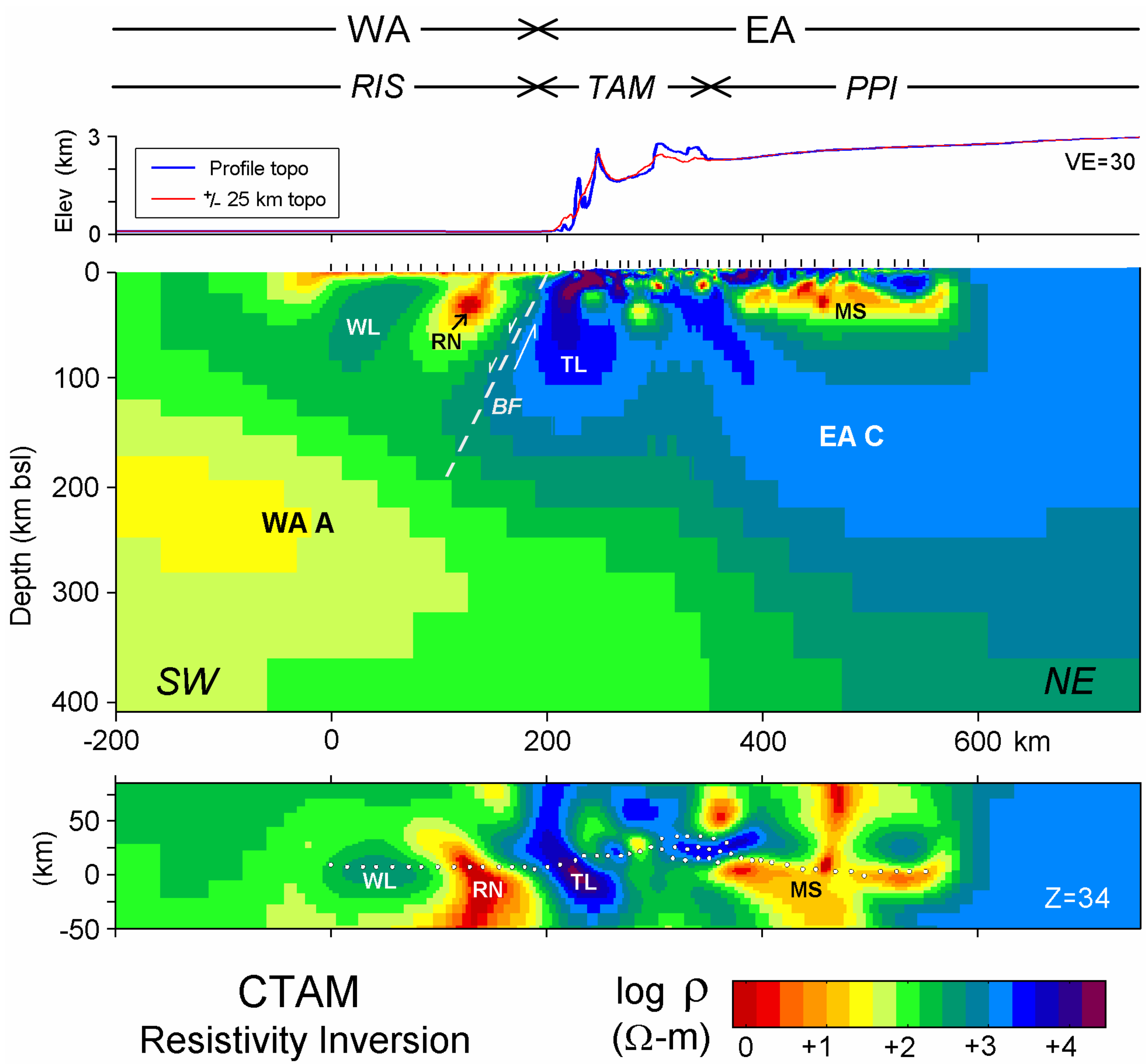

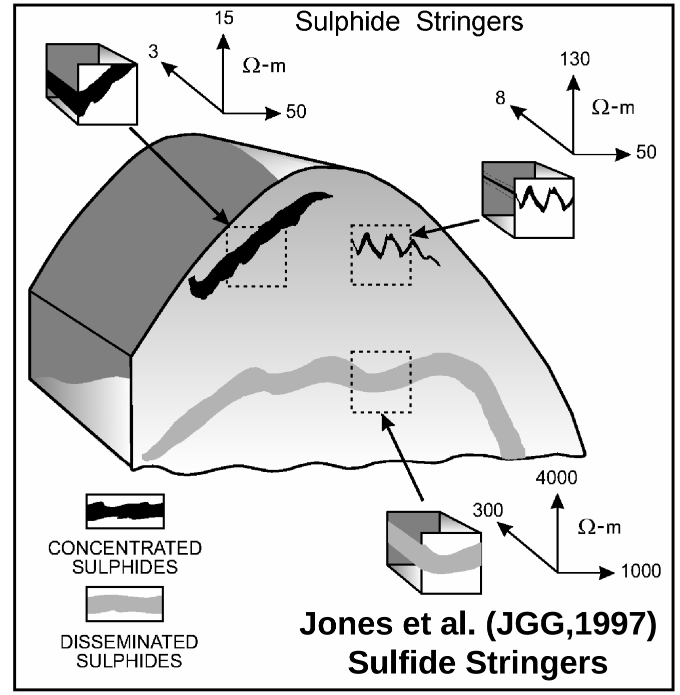

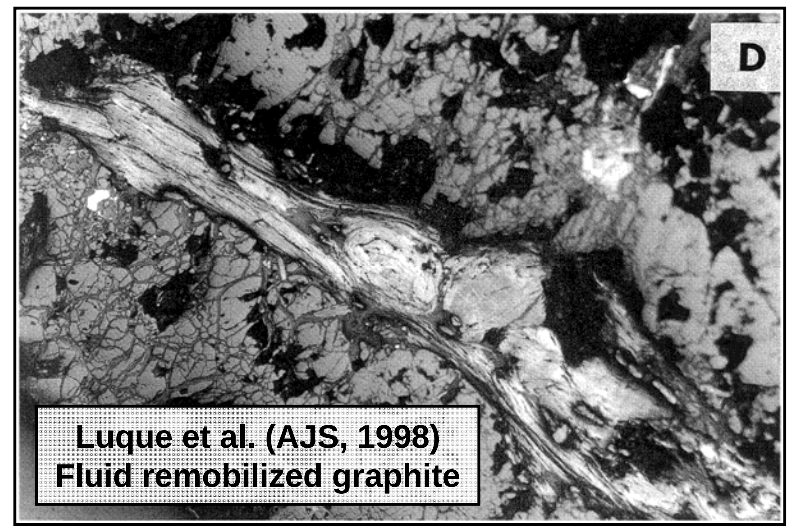

Graphite-sulfide textures in crustal-scale conductors

Goodge and Finn (2010): Crustal Architecture and Aeromagnetics

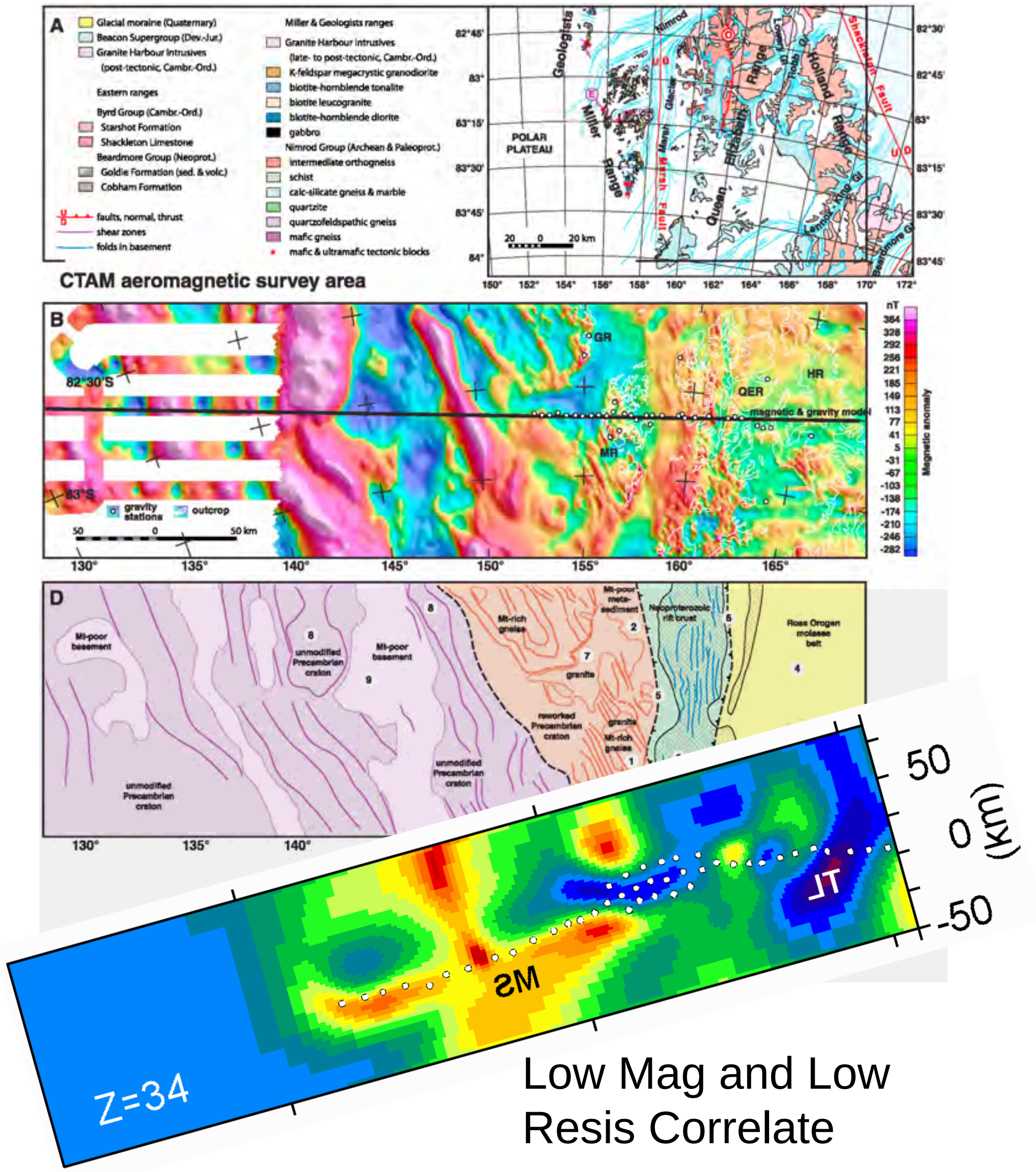

Low Mag and Low Resis Correlate

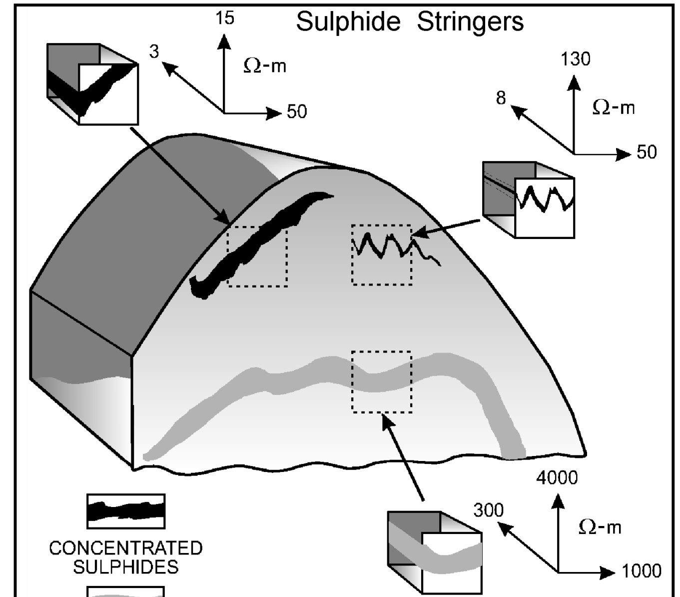

Jones et al. (JGG,1997) Sulfide Stringers

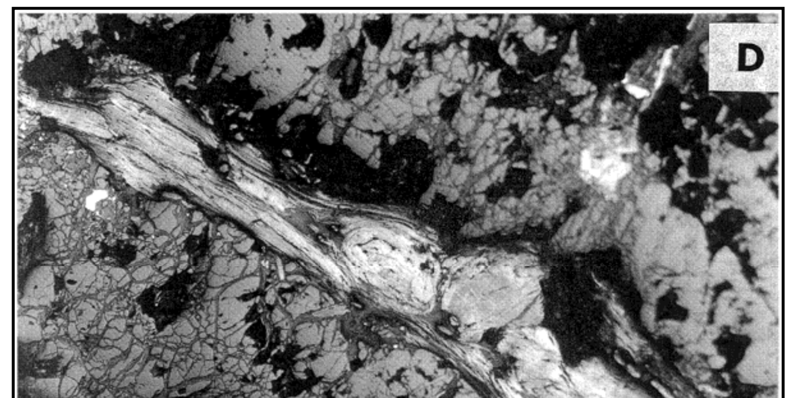

Luque et al. (AJS, 1998) Fluid remobilized graphite

Graphite-sulfide textures in crustal-scale conductors

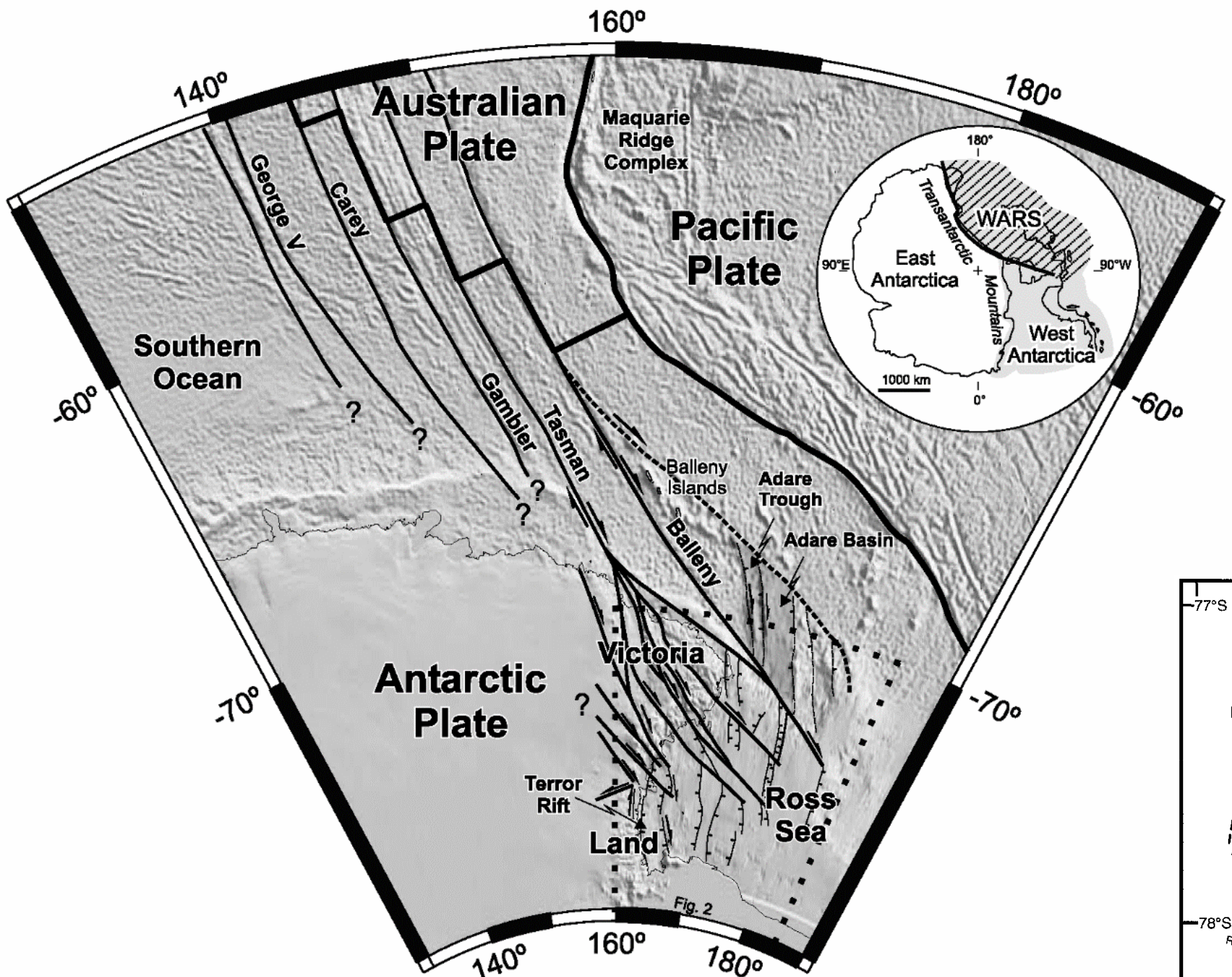

West Antarctic Rift System and Terror Magmatism (Faccenna et al., 2008; Storti et al., 2008)

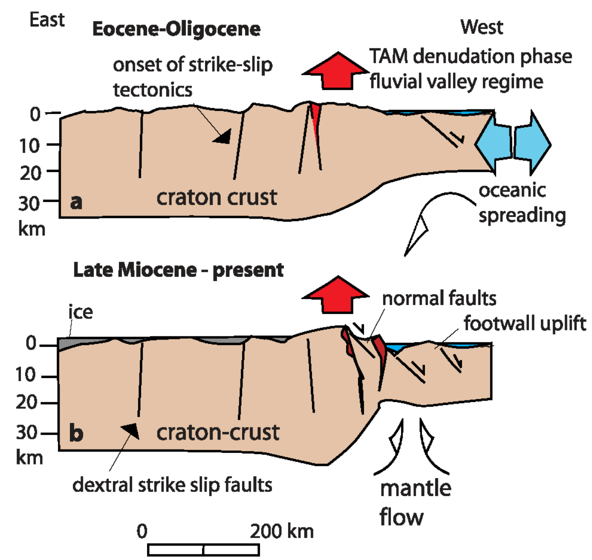

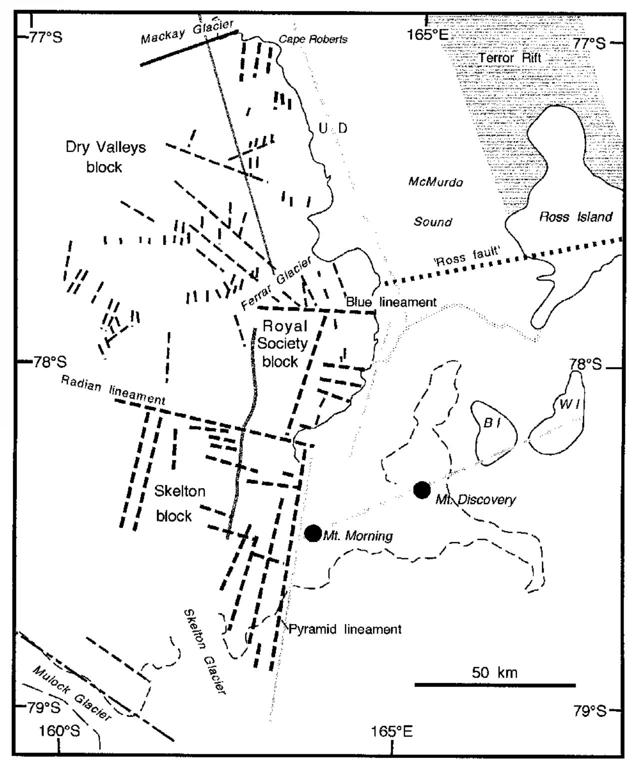

Discovery Accommodation Zone (Wilson, 1999)

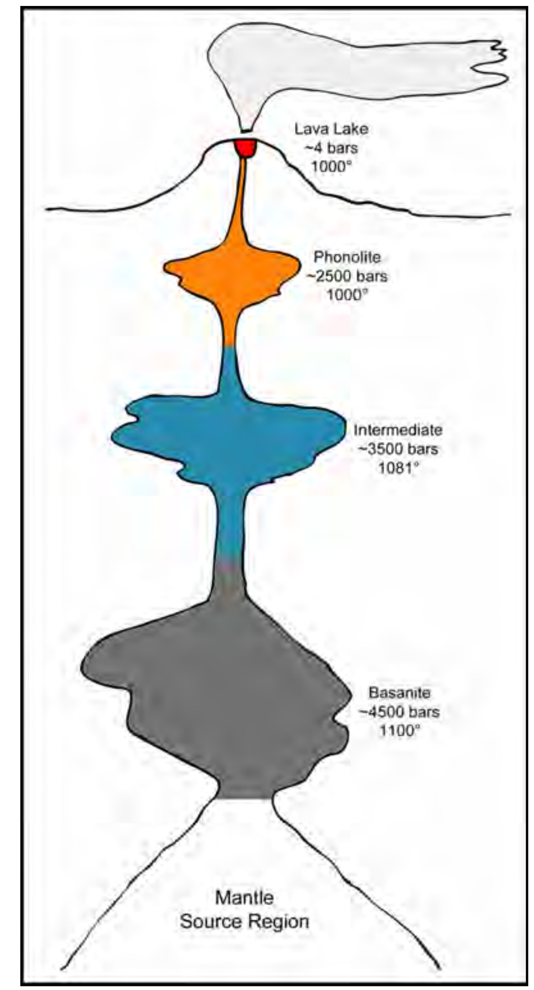

Mount Erebus Magma Source and Staging (Iacovino et al, 2015, after Oppenheimer, 2008)

Mount Erebus, Ross Island

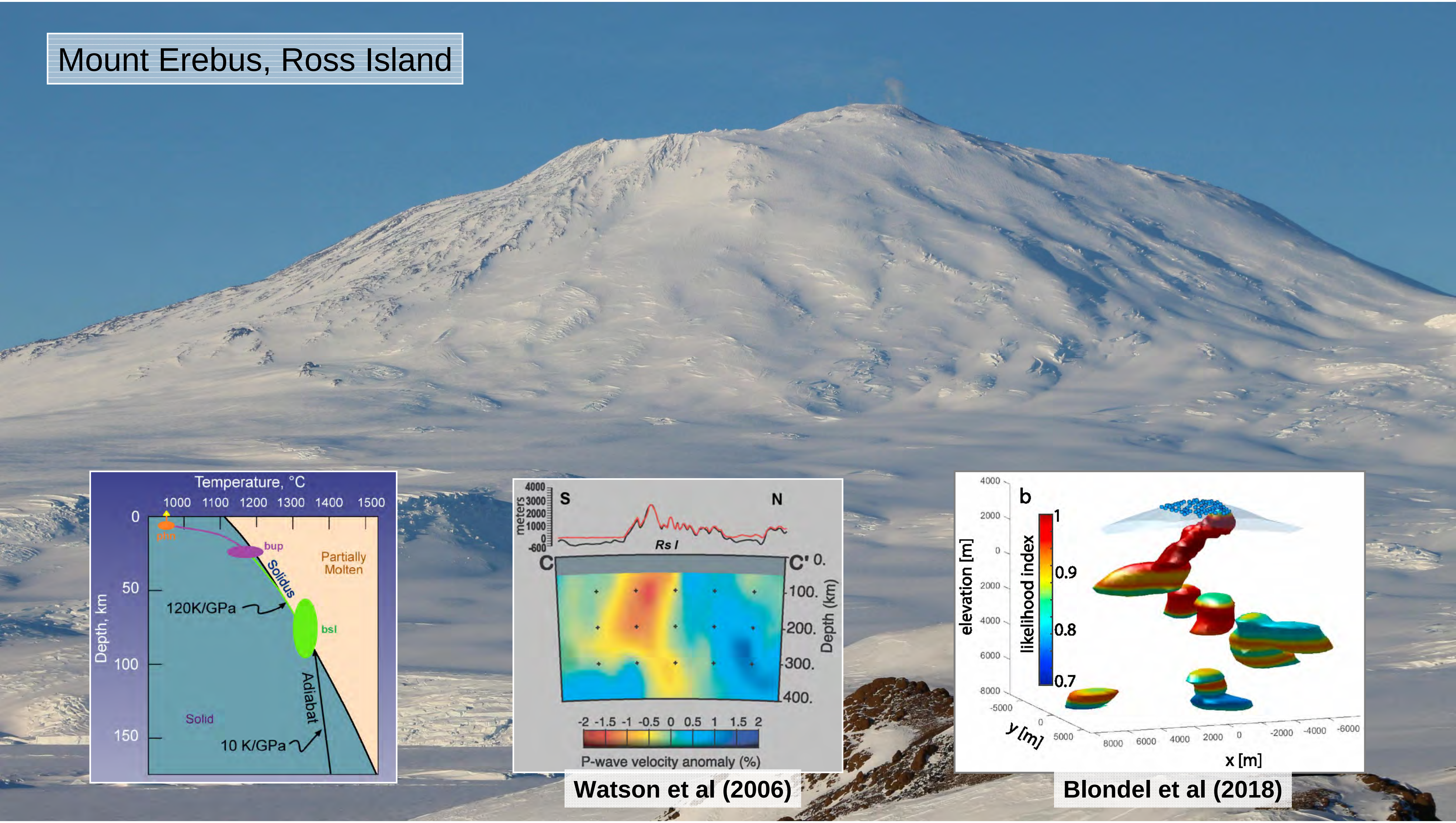

Watson et al (2006)

Blondel et al (2018)

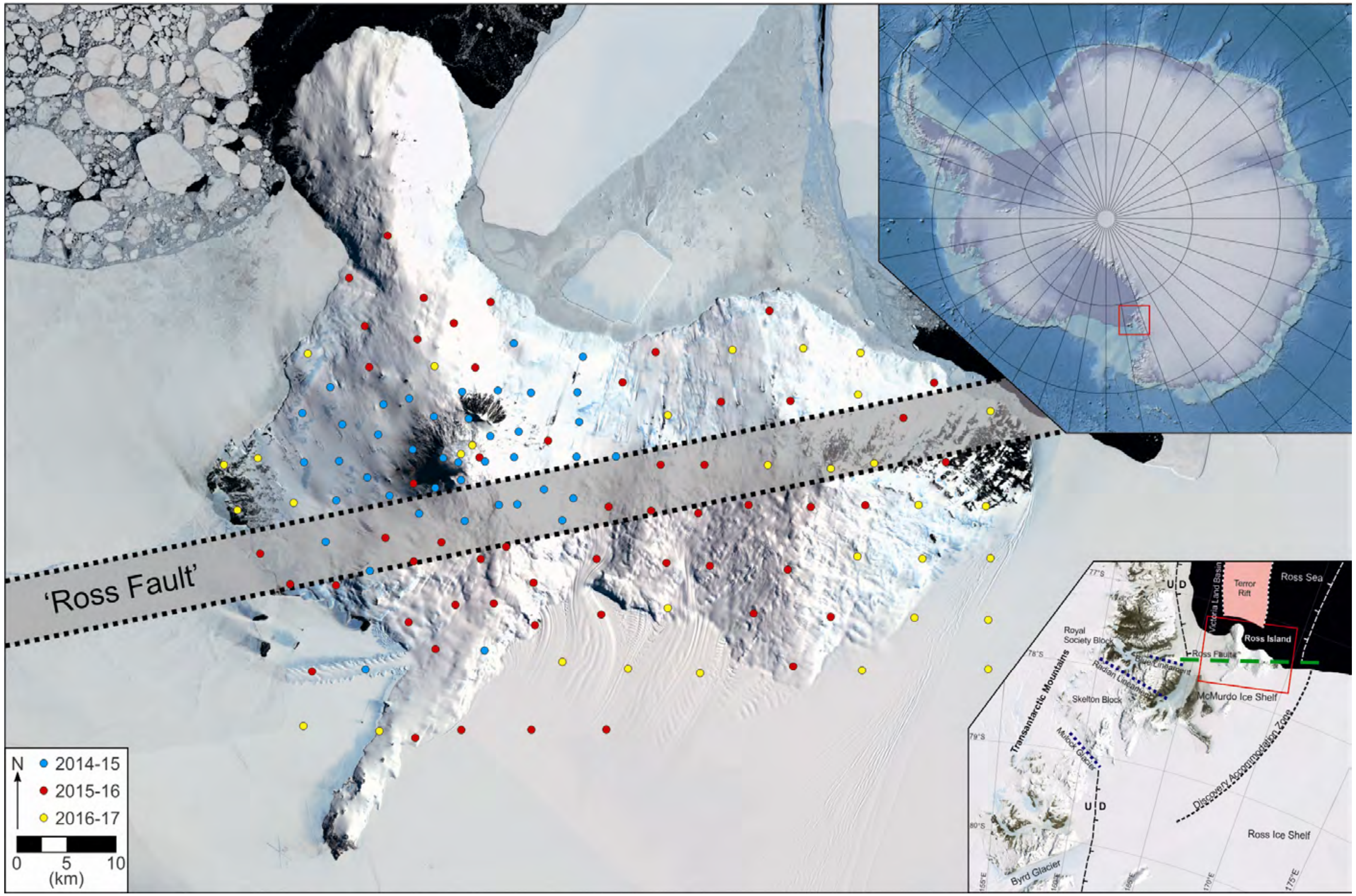

Mt Erebus MT Field Campaign: NSF/USAP and RSNZ/AntNZ

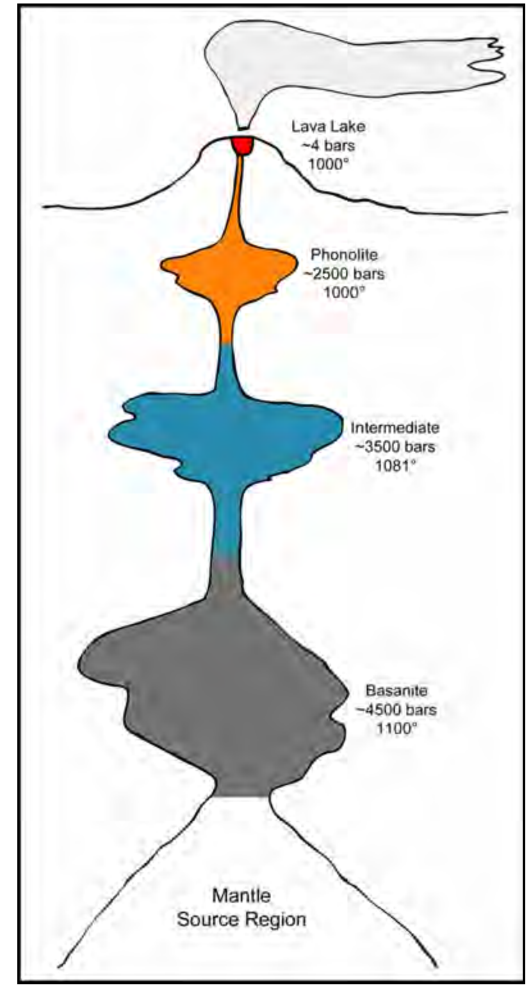

Mount Erebus Magma Source and Staging (Iacovino et al, 2015, after Oppenheimer, 2008)

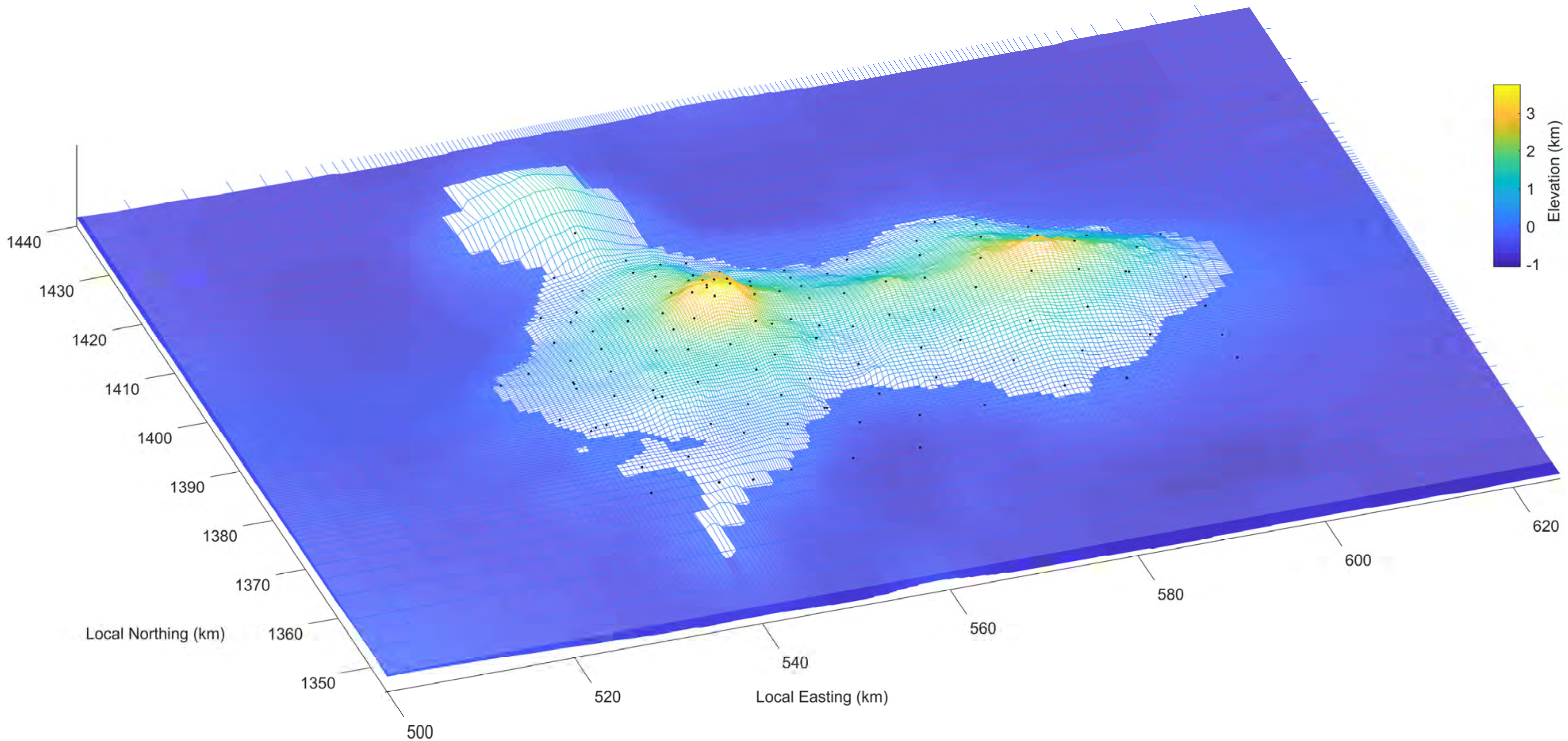

Mt Erebus MT Inversion Finite Element Mesh: ~1.4M cells

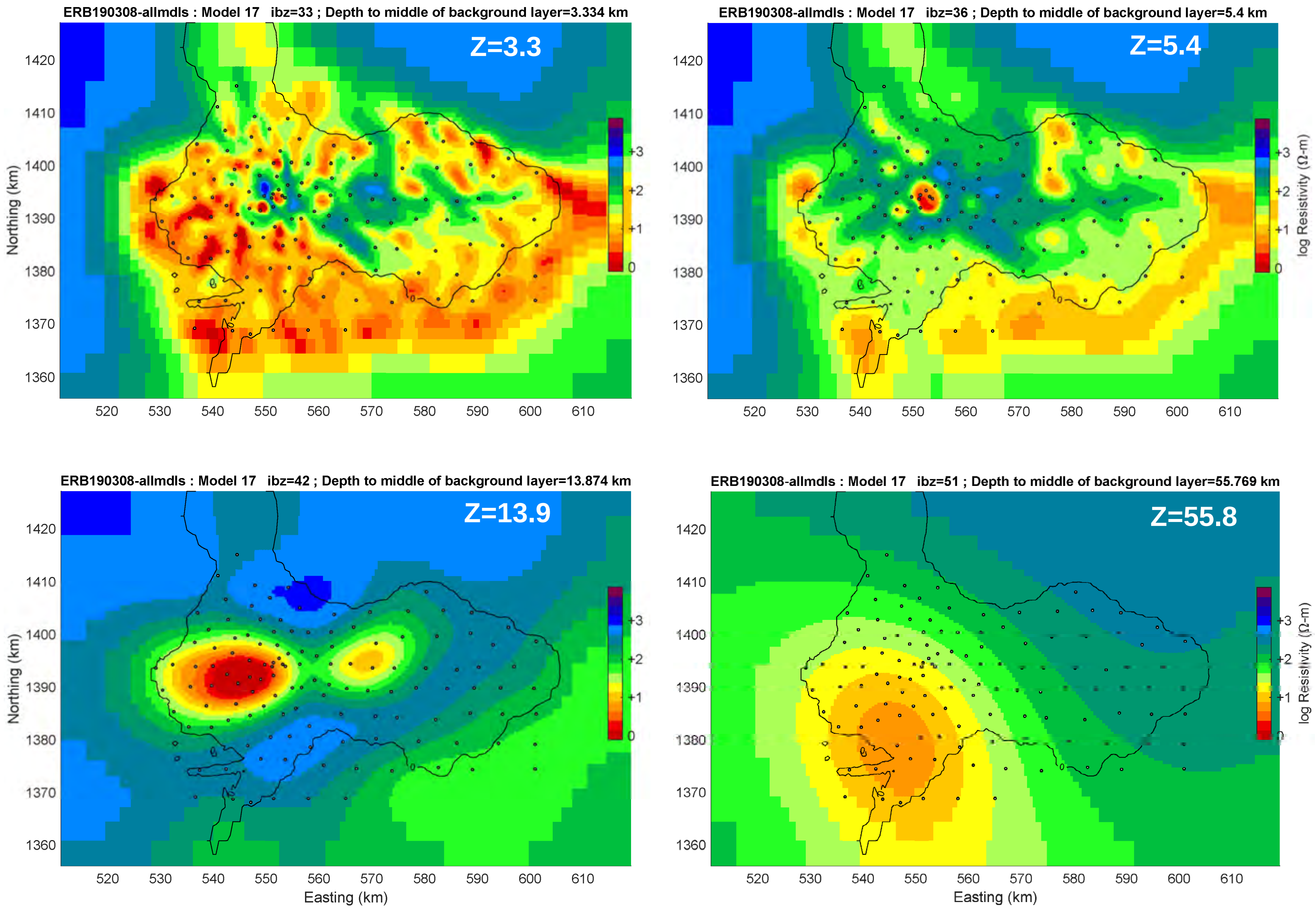

Mount Erebus MT Inversion Resistivity Plan Sections:

- General clay alteration blanket at shallow levels.

- Clear visibility of magmatic conduit and upper chamber by 5 km depth.

- migration of magmatic structure westward along apparent controlling E-W trend.

- Movement of magmatic plumbing southward from lower middle crust and deeper.

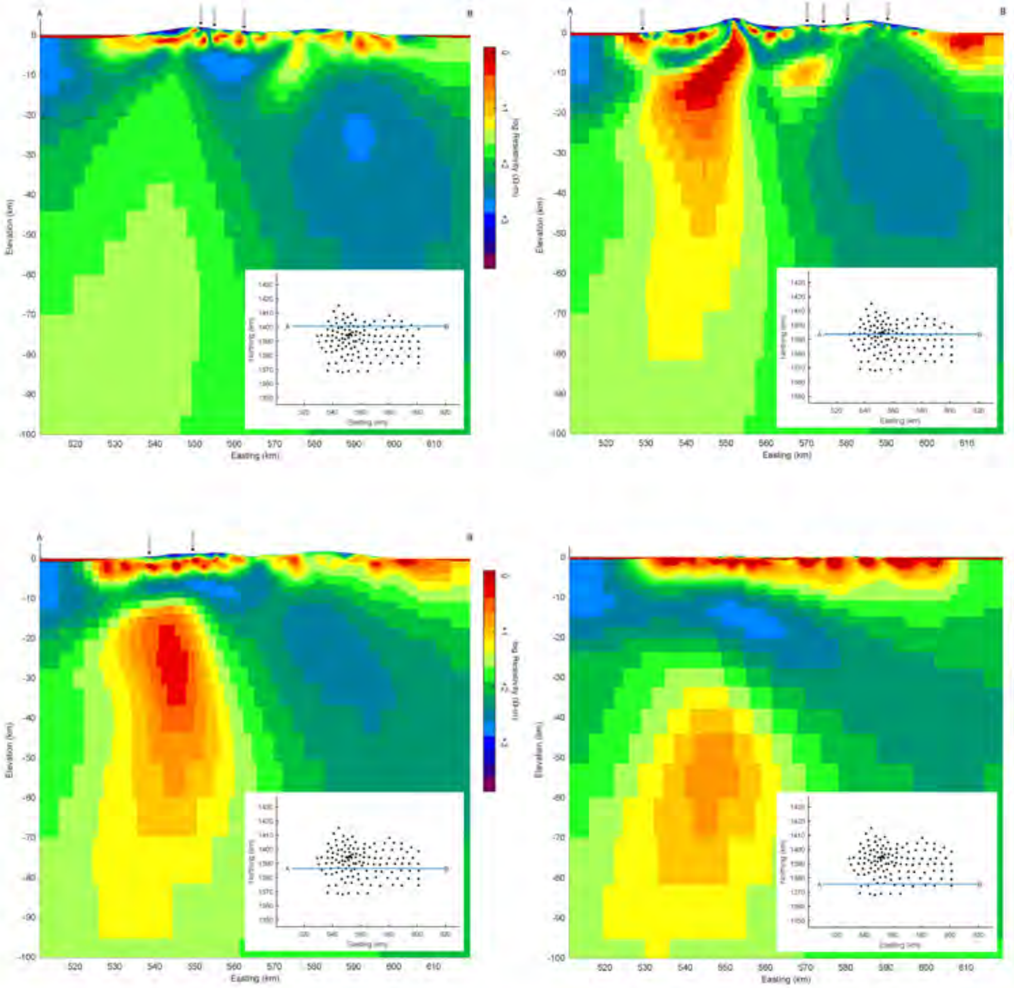

Mount Erebus MT Inversion Section
Views from East to West

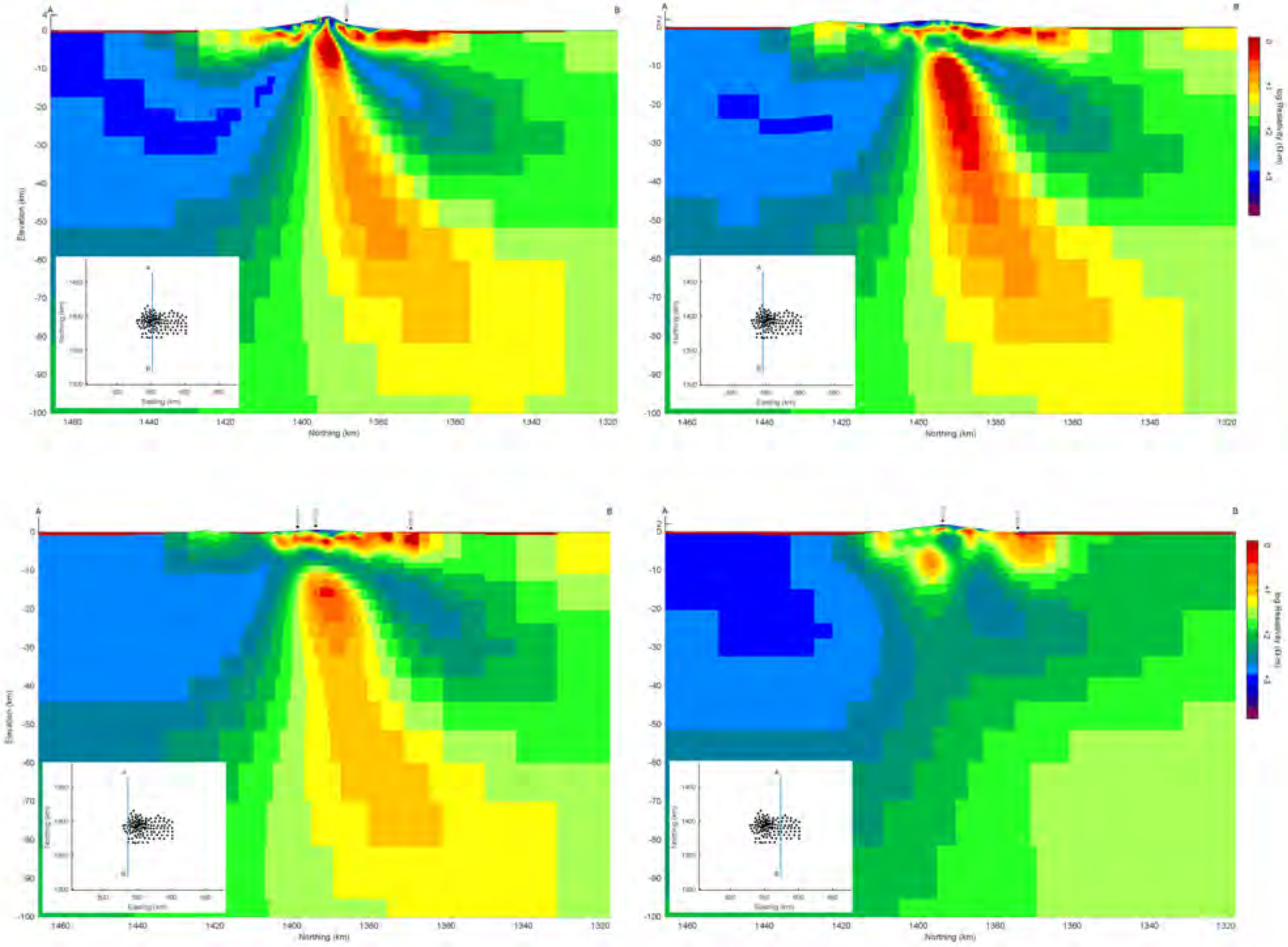

Mount Erebus MT Inversion Section
Views from North to South

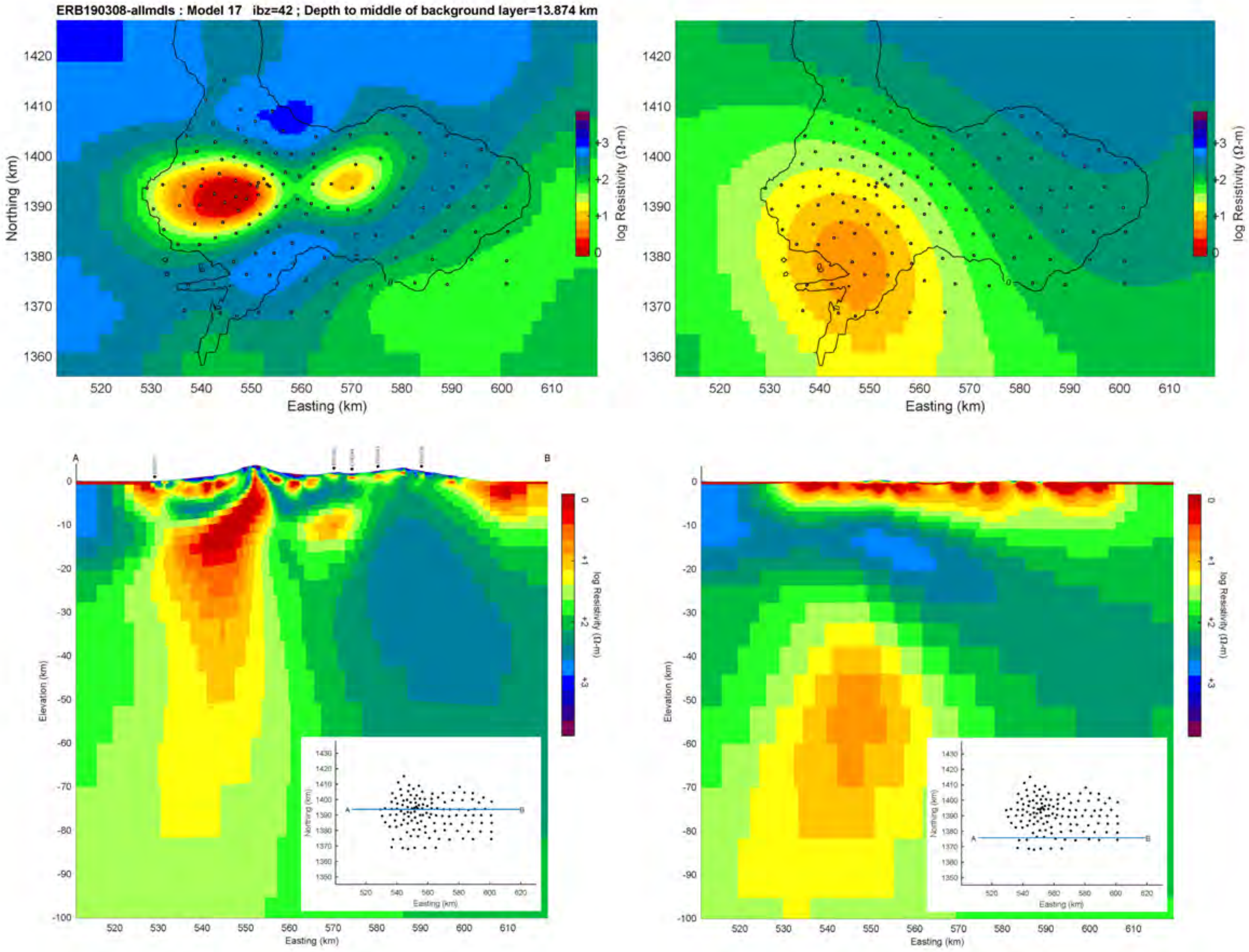

Mount Erebus MT Inversion Plan and Section Views

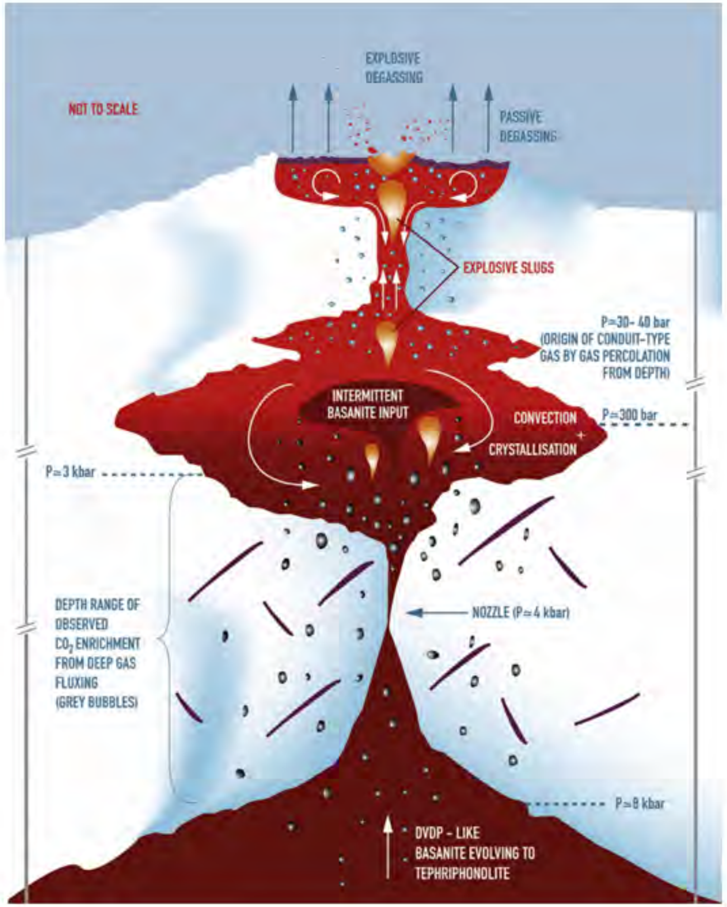

Schematic Mount Erebus magmatic plumbing (Oppenheimer et al., 2008). Note “Nozzle” interpreted at 4 kbar for periodic basanite replenishment.

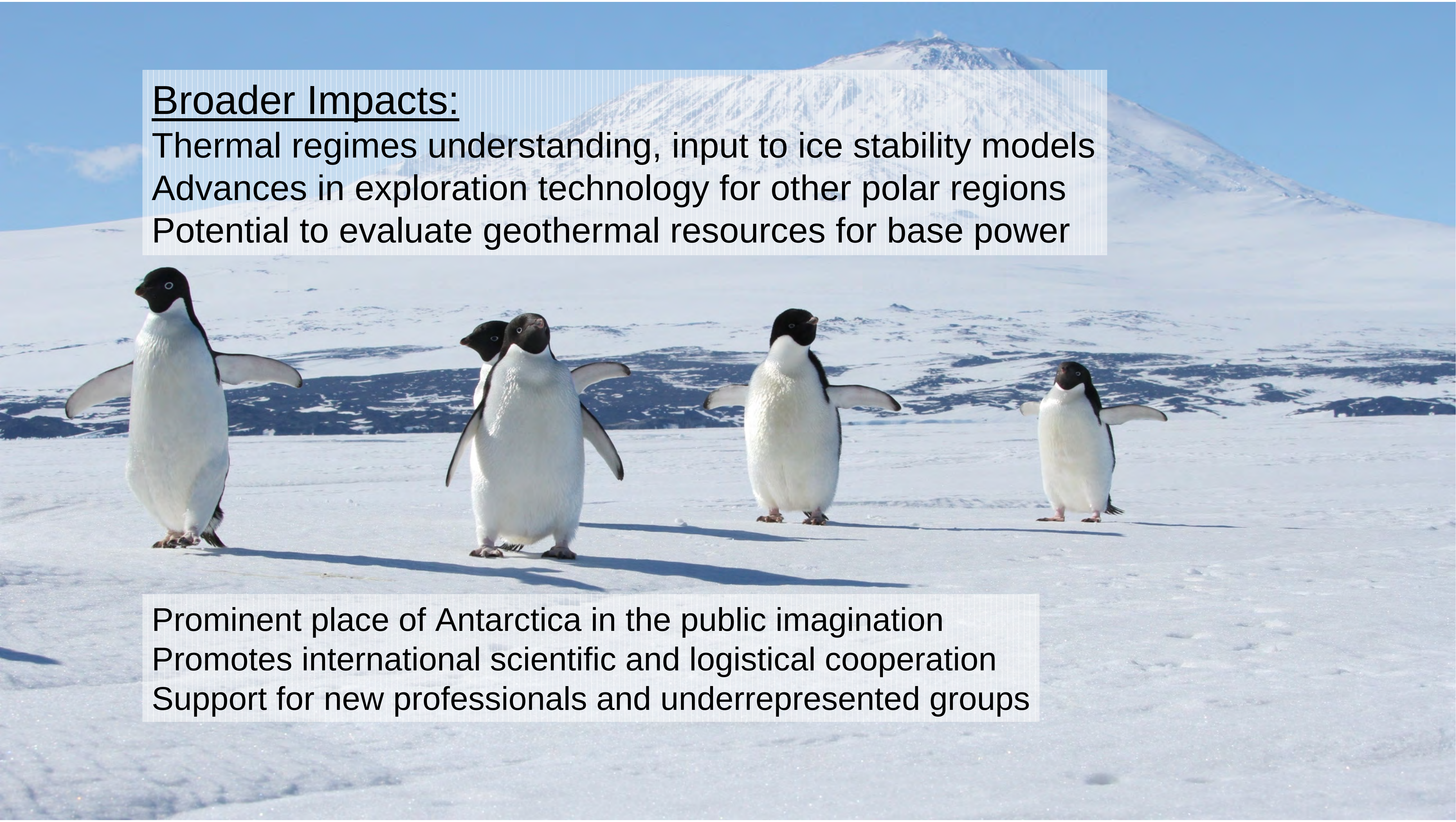

Broader Impacts:

Thermal regimes understanding, input to ice stability models
Advances in exploration technology for other polar regions
Potential to evaluate geothermal resources for base power

Prominent place of Antarctica in the public imagination
Promotes international scientific and logistical cooperation
Support for new professionals and underrepresented groups

The End!
MARSDEN FUND